Longitudinal changes in Alzheimer's-related plasma biomarkers and brain amyloid

Murat Bilgel[1], Yang An[1], Keenan A. Walker[1], Abhay R. Moghekar[2], Nicholas J. Ashton[3,4,5,6], Przemysław R. Kac[3], Thomas K. Karikari[3], Kaj Blennow[3], Henrik Zetterberg[3,7,8,9,10,11], Bruno M. Jedynak[12], Madhav Thambisetty[1], Luigi Ferrucci[13], Susan M. Resnick[1]

[1] Laboratory of Behavioral Neuroscience, National Institute on Aging, Baltimore, Maryland, USA

[2] Department of Neurology, Johns Hopkins University School of Medicine, Baltimore, Maryland, USA

[3] Department of Psychiatry and Neurochemistry, Institute of Neuroscience and Physiology, The Sahlgrenska Academy, University of Gothenburg, Mölndal, Sweden

[4] King's College London, Institute of Psychiatry, Psychology and Neuroscience, Maurice Wohl Clinical Neuroscience Institute, London, UK

[5] NIHR Biomedical Research Centre for Mental Health and Biomedical Research, Unit for Dementia at South London and Maudsley, NHS Foundation, London, UK

[6] Centre for Age-Related Medicine, Stavanger University Hospital, Stavanger, Norway

[7] Clinical Neurochemistry Laboratory, Sahlgrenska University Hospital, Mölndal, Sweden

[8] Department of Neurodegenerative Disease, UCL Institute of Neurology, Queen Square, London, UK

[9] UK Dementia Research Institute at UCL, London, UK

[10] Hong Kong Center for Neurodegenerative Diseases, Clear Water Bay, Hong Kong, China

[11] Wisconsin Alzheimer's Disease Research Center, University of Wisconsin School of Medicine and Public Health, University of Wisconsin-Madison, Madison, WI, USA

[12] Department of Mathematics and Statistics, Portland State University, Portland, Oregon, USA

[13] Translational Gerontology Branch, National Institute on Aging, Baltimore, Maryland, USA

Corresponding author: Murat Bilgel, murat.bilgel@nih.gov, 251 Bayview Blvd., Suite 100 Rm 04B329, Baltimore, MD, 21224 USA

Keywords: longitudinal; plasma; Pittsburgh compound B; positron emission tomography; biomarkers

Declarations of interest: MB, YA, KAW, ARM, NJA, PRK, TKK, BMJ, MT, LF, SMR: none

KB has served as a consultant, at advisory boards, or at data monitoring committees for Abcam, Axon, Biogen, JOMDD/Shimadzu, Julius Clinical, Lilly, MagQu, Novartis, Prothena, Roche Diagnostics, and Siemens Healthineers, and is a co-founder of Brain Biomarker Solutions in Gothenburg AB (BBS), which is a part of the GU Ventures Incubator Program (outside submitted work).

HZ has served at scientific advisory boards and/or as a consultant for Abbvie, Acumen, Alector, Alzinova, ALZPath, Annexon, Apellis, Artery Therapeutics, AZTherapies, CogRx, Denali, Eisai, Nervgen, Novo Nordisk, Optoceutics, Passage Bio, Pinteon Therapeutics, Prothena, Red Abbey Labs, reMYND, Roche, Samumed, Siemens Healthineers, Triplet Therapeutics, and Wave, has given lectures in symposia sponsored by Cellectricon, Fujirebio, Alzecure, Biogen, and Roche, and is a co-founder of Brain Biomarker Solutions in Gothenburg AB (BBS), which is a part of the GU Ventures Incubator Program (outside submitted work).

Abstract

Introduction: Understanding longitudinal plasma biomarker trajectories relative to brain amyloid changes can help devise disease progression assessment strategies for Alzheimer's disease.

Methods: We examined the temporal order of changes in plasma amyloid-β ratio ($A\beta_{42}/A\beta_{40}$), glial fibrillary acidic protein (GFAP), neurofilament light chain (NfL), and two phosphorylated tau ratios (p-tau181/$A\beta_{42}$ and p-tau231/$A\beta_{42}$) relative to ^{11}C-Pittsburgh compound B (PiB) positron emission tomography (PET) cortical amyloid burden (PiB−/+). Participants (n = 199, Baltimore Longitudinal Study of Aging) were cognitively normal at index visit with a median 6.1-year follow-up.

Results: PiB− individuals exhibited longitudinal decline in $A\beta_{42}/A\beta_{40}$ ($\beta = -3.85 \times 10^{-4}$, SE = 9.77×10^{-5}, $p = 1.96 \times 10^{-4}$), whereas PiB+ did not exhibit change. Change in brain amyloid was correlated with change in GFAP (r = 0.5, 95% CI = [0.26, 0.68]) and NfL (r = 0.4 [0.13, 0.62]). Greatest relative decline in $A\beta_{42}/A\beta_{40}$ (-1% per year) preceded brain amyloid positivity onset by 41 years (95% CI = [32, 53]).

Discussion: Plasma $A\beta_{42}/A\beta_{40}$ may begin declining decades prior to brain amyloid, whereas p-tau ratio, GFAP, and NfL increase closer in time to, and in parallel with, brain amyloid accumulation.

Highlights:

- Plasma $A\beta_{42}/A\beta_{40}$ declines over time among PiB− but does not change among PiB+
- p-tau to $A\beta_{42}$ ratios increase over time among PiB+ but do not change among PiB−
- Rate of change in brain amyloid is correlated with change in GFAP and NfL
- Greatest decline in $A\beta_{42}/A\beta_{40}$ may precede brain amyloid positivity by decades

1 Background

Plasma biomarkers of Alzheimer's disease (AD)-related pathology and neurodegeneration are proxies of these changes in the central nervous system. Their low cost and ease of collection make them good candidates for widespread clinical use for assessing AD-related changes.

Amyloid-β (Aβ) accumulation marks the beginning of preclinical Alzheimer's among cognitively unimpaired individuals [1]. As highlighted in the research priorities outlined by Hansson et al. [2], it is important to understand longitudinal changes in plasma biomarkers in relation to the onset of this hallmark neuropathology. A better understanding of longitudinal plasma biomarker trajectories can allow for patient selection and monitoring in clinical trials, facilitating identification of individuals at high risk of developing neurodegenerative changes and cognitive impairment. Plasma biomarkers may be particularly useful in limiting the number of positron emission tomography (PET) scans conducted to determine participant eligibility for trials of anti-amyloid treatments [3–7].

Despite the rapidly developing research on plasma biomarkers, studies investigating longitudinal change remain limited. Chatterjee et al. reported that plasma measures of $A\beta_{42}/A\beta_{40}$, tau phosphorylated at threonine 181 (p-tau181), and glial fibrillary acidic protein (GFAP) change more rapidly among individuals with mild cognitive impairment (MCI) compared to cognitively normal individuals [8]. O'Connor et al. found that longitudinal trajectories of plasma neurofilament light chain (NfL) and p-tau181 among autosomal dominant AD mutation carriers started diverging from trajectories observed for non-carriers at about 16–17 years prior to estimated symptom onset [9]. Plasma

$A\beta_{42}/A\beta_{40}$ [10] and p-tau181 [11] have also been shown to exhibit changes prior to elevated brain amyloid levels, with plasma Aβ changing prior to p-tau181 [12]. In a cohort that included individuals with and without cognitive impairment, Rauchmann et al. examined trajectories of plasma p-tau181 and NfL relative to cerebrospinal fluid or imaging measure-based definitions of amyloid (A), tau (T), and neurodegeneration (N) status and found that relative to the A−TN− group, all other groups exhibited steeper longitudinal increases in NfL [13]. Further, recent cross-sectional and longitudinal studies have shown early changes of all plasma biomarkers but note that p-tau231 changes earliest in response to Aβ deposition [14–16]. These findings suggest that these plasma biomarkers may be dynamic in the preclinical phase of AD and even earlier. However, it remains unclear how closely longitudinal changes in plasma biomarkers mirror longitudinal changes in brain amyloid levels and when changes in plasma biomarkers begin and peak relative to changes in brain amyloid levels.

In this study, we focus on understanding the temporal order of changes in AD-related plasma biomarkers relative to brain amyloid levels as measured with ^{11}C-Pittsburgh compound B (PiB) PET. The plasma measures we consider include $A\beta_{42}$, $A\beta_{40}$, GFAP, NfL, p-tau181, and p-tau231 as well as the ratios $A\beta_{42}/A\beta_{40}$, p-tau181/$A\beta_{42}$, and p-tau231/$A\beta_{42}$. We first examine plasma biomarkers cross-sectionally to replicate previous findings regarding their accuracy in classifying amyloid PET status. We then use longitudinal plasma biomarker data to quantify their longitudinal intraclass correlation coefficients, estimate their trajectories as a function of brain amyloid status, investigate the associations among longitudinal rates of change in plasma and brain amyloid measures, and finally, examine the temporal order of changes in plasma measures relative to brain amyloid.

2 Methods

2.1 Participants

Our sample consisted of 199 Baltimore Longitudinal Study of Aging (BLSA) participants with amyloid PET scans and plasma biomarker measurements. Measurements at the index visit, defined as the earliest cognitively normal visit with a full set of plasma biomarker measurements, were used to conduct cross-sectional analyses. All available plasma biomarker measurements for these participants were used in longitudinal analyses, allowing for inclusion of visits where a subset of plasma biomarker measurements was missing (because measurement was not performed or did not meet quality control).

Research protocols were conducted in accordance with United States federal policy for the protection of human research subjects contained in Title 45 Part 46 of the Code of Federal Regulations, approved by local institutional review boards, and all participants gave written informed consent at each visit.

2.2 Cognitive assessment

Cognitively normal status was based on either (i) three or fewer errors on the Blessed Information-Memory-Concentration Test [17] and a Clinical Dementia Rating [18] of zero, or (ii) the participant was determined to be cognitively normal based on thorough review of clinical and neuropsychological data at consensus diagnostic conference. MCI and dementia diagnoses were determined according to Petersen [19] and Diagnostic and Statistical Manual of Mental Disorders III-R criteria [20], respectively.

2.3 PET image acquisition and processing

Dynamic amyloid PET scans were acquired using the ^{11}C-PiB radiotracer over 70 min on either a General Electric Advance scanner or a Siemens High Resolution Research Tomograph immediately following an intravenous bolus injection of approximately 555 MBq of radiotracer. Distribution volume ratio (DVR) was calculated using a spatially constrained simplified reference tissue model with a cerebellar gray matter reference region [21]. Mean cortical amyloid burden was calculated as the average DVR in the cingulate, frontal, parietal (including precuneus), lateral temporal, and lateral occipital regions, excluding the pre- and post-central gyri. Mean cortical DVR (cDVR) values were harmonized between the two scanners by leveraging longitudinal data available on both scanners for 79 participants. PET acquisition and processing are described in detail in Bilgel et al. [22,23]. The number of longitudinal PiB PET measurements included was 589.

2.3.1 PiB group determination

PiB PET scans were categorized as −/+ based on a cDVR threshold of 1.06 derived from a Gaussian mixture model fitted to harmonized cDVR values at first PET. We imputed PiB group for visits without a PiB PET scan (Supplementary Material).

2.4 Plasma biomarkers

$A\beta_{40}$, $A\beta_{42}$, GFAP, and NfL were measured at Johns Hopkins University (Baltimore, Maryland, USA) on a Quanterix (Billerica, Massachusetts, USA) HD-X instrument using the Quanterix Simoa Neurology 4-plex-E assay in duplicate and averaged (intra-assay

coefficient of variation was 2.8, 1.9, 5.0, and 5.1, respectively [24]). Three outlying NfL measurements >125 pg/mL were excluded based on examination of within-individual longitudinal data. p-tau181 and p-tau231 were measured at the Clinical Neurochemistry Laboratory, University of Gothenburg (Mölndal, Sweden) on a Quanterix HD-X instrument using assays developed in-house [25,26]. Repeatability coefficient was 5.1% and 5.5% for the p-tau181 assay at a concentration of 11.6 and 15.5 pg/mL, respectively. Repeatability coefficient was 3.4% and 7.4% for the p-tau231 assay at a concentration of 31.6 and 42.7 pg/mL, respectively. For the p-tau measures, values below limit of quantitation were imputed at 0 and values below lower limit of detection were kept as is. In addition to individual protein levels, we also investigated the ratios $A\beta_{42}/A\beta_{40}$, p-tau181/$A\beta_{42}$, and p-tau231/$A\beta_{42}$. The number of longitudinal measurements included was 685 for $A\beta_{40}$, $A\beta_{42}$ and GFAP, 682 for NfL, 671 for p-tau181, 676 for p-tau231, 597 for p-tau181/$A\beta_{42}$, and 602 for p-tau231/$A\beta_{42}$.

We estimated glomerular filtration rate (eGFR) at each plasma visit from serum creatinine levels using the Chronic Kidney Disease-Epidemiology collaboration formula. For visits without serum creatinine measurements, we imputed eGFR by carrying the eGFR measurement forward or backward in time within person.

2.5 Statistical analysis

2.5.1 Classification of brain amyloid status using plasma biomarkers

We assessed the performance of each plasma measure in classifying individuals into PiB groups in our cross-sectional dataset. We examined the receiver operating characteristic

(ROC) curve and the area under the curve (AUC) separately for each measure. We also assessed how well the plasma measures and demographics (age, sex, race, and *APOE* $\varepsilon 4$ genotype) performed in multivariable analyses for classifying PiB group. Unlike univariable analyses, multivariable analyses involved estimating model parameters. Because of this, we used 10-fold stratified (i.e., the proportion of PiB+ individuals in each fold was approximately the same) cross-validation to obtain ROC curves by estimating model parameters in the training set and obtaining predictions in the testing set. The models investigated included elastic net logistic regression models (with varying levels of ℓ_1 and ℓ_2 penalties to span the spectrum from Lasso to ridge regression), distributed random forests, gradient boosting machines, and extreme gradient boosting (XGBoost). Multivariable classifiers were fitted using the `automl` function in the `H2O` package (version 3.36.0.3) [27,28] in R version 4.0.3 [29] with a range of hyperparameter combinations for each classifier.

2.5.2 Longitudinal intraclass correlation coefficients

We computed longitudinal intraclass correlation coefficients (ICC) using a linear mixed effects model (LMEM) for each biomarker that included an intercept and time from index visit term as fixed effects and a random intercept per participant. ICC was calculated as the ratio of the variance of the random intercept to the sum of the variances of the random intercept and noise. We calculated longitudinal ICC using data for (i) all, (ii) only PiB−, and (iii) only PiB+ individuals.

2.5.3 Longitudinal plasma biomarker trajectories by brain amyloid status

We examined the longitudinal plasma biomarker trajectories by brain amyloid status using a separate LMEM per biomarker. Unadjusted models included PiB group at index visit, time from index visit, and their interaction. Adjusted models additionally included age at index visit, sex, race, *APOE* $\varepsilon 4$ carrier vs. non-carrier status, and age × time interaction. We also included eGFR and body mass index (BMI) concurrent with plasma measurement as covariates given their associations with plasma biomarker levels [30].

2.5.4 Associations among longitudinal rates of change in plasma biomarkers and brain amyloid

We used bivariate LMEMs to examine the association between the rates of change in pairs of biomarkers. We considered the longitudinal data for two biomarkers simultaneously as dependent variables. Independent variables were age at index visit, time from index visit, age × time interaction, sex, race, and *APOE* $\varepsilon 4$ status. For plasma biomarkers, we additionally adjusted for eGFR and BMI concurrent with plasma measurement. We estimated a separate noise variance for each outcome. We included a random intercept and slope over time per participant for each of the outcomes, and the covariance of these four random effects was modeled using an unstructured covariance matrix. The correlation matrix was extracted from the estimated covariance. We examined the correlation between random slopes to assess the association between rates of biomarker change. Bivariate LMEMs were fitted using the `lme` function and confidence intervals for the correlation parameters were computed using the `intervals` function in the `nlme` package [31].

2.5.5 Temporal order of changes in plasma biomarkers and brain amyloid

We assessed the temporal order of changes in plasma biomarkers using a Bayesian implementation of the progression score (PS) model (modified from [32]). The PS model accounts for individual differences in the onset of biomarker changes by estimating a time-shift per individual to better align biomarker measurements. We modeled the trajectories of plasma biomarkers and cDVR using sigmoid functions. This analysis was limited to 577 longitudinal visits where the full set of plasma biomarkers and cDVR were available.

Since cognitive diagnosis is not used in the PS model, we used it to check that the resulting progression scores are meaningful (i.e., higher PS among individuals with MCI or dementia) and that the PS reflects more information than age in its association with cognitive diagnosis. At the last visit, we compared PS and the time-shift variable τ between cognitively normal individuals and those with MCI or dementia.

3 Results

3.1 Descriptives

Participant demographics are presented in Table 1. Compared to PiB−, PiB+ individuals were more likely to be *APOE* $\varepsilon 4$ carriers, had lower plasma $A\beta_{42}/A\beta_{40}$, higher $A\beta_{40}$, p-tau181, p-tau231, p-tau181/$A\beta_{42}$, p-tau231/$A\beta_{42}$, GFAP, and NfL at index visit, and were less likely to remain cognitively normal. At index visit, eGFR was positively correlated with $A\beta_{42}/A\beta_{40}$ ($r = 0.18$, 95% CI = [0.039, 0.31], $p = 0.013$) and negatively correlated with the remaining plasma measures (r ranging from -0.45 to -0.17, all $p < 0.018$). BMI was

negatively correlated with p-tau181/Aβ_{42} (r = -0.14, 95% CI = [-0.28, -0.0044], p = 0.043), GFAP (r = -0.28, 95% CI = [-0.41, -0.15], $p = 5.17 \times 10^{-5}$), and NfL (r = -0.27, 95% CI = [-0.4, -0.14], $p = 8.60 \times 10^{-5}$). Men had lower Aβ_{42}/Aβ_{40} and higher Aβ_{40}, p-tau181, p-tau231, p-tau181/Aβ_{42}, p-tau231/Aβ_{42}, GFAP, and NfL compared to women. White participants had higher p-tau181, p-tau181/Aβ_{42}, GFAP, and NfL compared to Non-White participants. Relationships of plasma and PiB PET measures with eGFR, BMI, sex, and race are shown in Supplementary Figures 1–4. We did not observe any associations of eGFR, BMI, sex, or race with PiB cDVR. Correlations among plasma and PiB PET measures at index visit are presented in Supplementary Figure 5 and longitudinal measures versus age in Supplementary Figure 6.

Table 1: Participant characteristics. *Time-varying variables are summarized at the index visit. For continuous and categorial variables, we report the median and interquartile range and the N and percentage, respectively. PiB group comparisons are based on Wilcoxon rank-sum test for continuous variables and Pearson's Chi-squared test or Fisher's exact test for categorical variables.*

Characteristic	Overall, N = 199	PiB-, N = 141	PiB+, N = 58	p-value
Age (yr)	76 (69, 82)	74 (68, 81)	79 (73, 84)	0.005
Male	97 (49%)	66 (47%)	31 (53%)	0.4
Race				>0.9
API and Other	9 (4.5%)	7 (5.0%)	2 (3.4%)	
Black	34 (17%)	25 (18%)	9 (16%)	
White	156 (78%)	109 (77%)	47 (81%)	
APOE ε4+	59 (30%)	36 (26%)	23 (40%)	0.047

Characteristic	Overall, N = 199	PiB-, N = 141	PiB+, N = 58	p-value
eGFR (mL/min/1.73 m^2)	73 (63, 85)	74 (64, 86)	72 (59, 79)	0.079
BMI (kg/m^2)	26.7 (24.2, 30.1)	27.4 (24.2, 31.1)	26.3 (24.2, 29.0)	0.2
$A\beta_{42}/A\beta_{40}$	0.050 (0.044, 0.056)	0.052 (0.047, 0.060)	0.046 (0.040, 0.051)	<0.001
p-tau181/$A\beta_{42}$	1.11 (0.77, 1.72)	0.93 (0.70, 1.43)	1.71 (1.28, 2.89)	<0.001
p-tau231/$A\beta_{42}$	2.51 (1.87, 3.56)	2.22 (1.81, 2.99)	4.05 (2.62, 5.94)	<0.001
GFAP (pg/mL)	185 (131, 251)	173 (122, 217)	229 (185, 301)	<0.001
NfL (pg/mL)	23 (17, 31)	22 (16, 28)	27 (20, 36)	0.002
$A\beta_{40}$	139 (114, 169)	133 (111, 163)	150 (123, 184)	0.011
$A\beta_{42}$	6.95 (5.62, 8.16)	7.24 (5.67, 8.17)	6.48 (5.51, 7.84)	0.2
p-tau181	7 (5, 11)	7 (5, 9)	11 (8, 18)	<0.001
p-tau231	18 (13, 24)	16 (13, 20)	27 (16, 36)	<0.001
Hypertension	107 (54%)	83 (59%)	24 (41%)	0.025
Diabetes	38 (19%)	26 (18%)	12 (21%)	0.7
High cholesterol	114 (57%)	84 (60%)	30 (52%)	0.3
Obesity	53 (27%)	44 (31%)	9 (16%)	0.023
Smoking				0.5
Never	101 (52%)	73 (53%)	28 (50%)	
Former	90 (46%)	62 (45%)	28 (50%)	
Current	4 (2.1%)	4 (2.9%)	0 (0%)	
Unknown	4	2	2	
Number of visits	3 (2, 5)	3 (2, 5)	4 (2, 5)	0.8
Follow-up duration (yr)	6.1 (4.0, 8.6)	6.1 (4.0, 8.6)	6.1 (3.8, 8.7)	0.6
Final diagnosis				0.001
Cognitively normal	157 (79%)	121 (86%)	36 (62%)	
MCI	20 (10%)	9 (6.4%)	11 (19%)	
Other impairment	1 (0.5%)	0 (0%)	1 (1.7%)	
Dementia	21 (11%)	11 (7.8%)	10 (17%)	

Abbreviations: Aβ, amyloid-β; API, Asian/Pacific Islander; *APOE*, apolipoprotein E; BMI, body mass index; eGFR, estimated glomerular filtration rate; GFAP, glial fibrillary acidic protein; MCI, mild cognitive impairment; NfL, neurofilament light chain; PiB, Pittsburgh compound B; p-tau, phosphorylated tau.

3.2 Classification of brain amyloid status using plasma biomarkers

3.2.1 Univariate models based on a single plasma biomarker or biomarker ratio

ROC curves for the univariate models are presented in Figure 1 and Supplementary Figure 7. The best univariate classifiers were p-tau231/Aβ_{42}, p-tau181/Aβ_{42}, and p-tau231, with AUCs in the range 0.76–0.78 (Supplementary Table 1). The performance of the NfL-only classifier (AUC = 0.64, 95% CI = [0.55–0.72]) was similar to that of the age-only classifier (AUC = 0.63, 95% CI = [0.54–0.71]), whereas Aβ_{42}/Aβ_{40} (AUC = 0.72, 95% CI = [0.65–0.79]), p-tau181 (AUC = 0.72, 95% CI = [0.63–0.8]), p-tau231 (AUC = 0.76, 95% CI = [0.67–0.85]), p-tau181/Aβ_{42} (AUC = 0.77, 95% CI = [0.7–0.84]), p-tau231/Aβ_{42} (AUC = 0.78, 95% CI = [0.71–0.86]), and GFAP (AUC = 0.71, 95% CI = [0.63–0.79]) outperformed age.

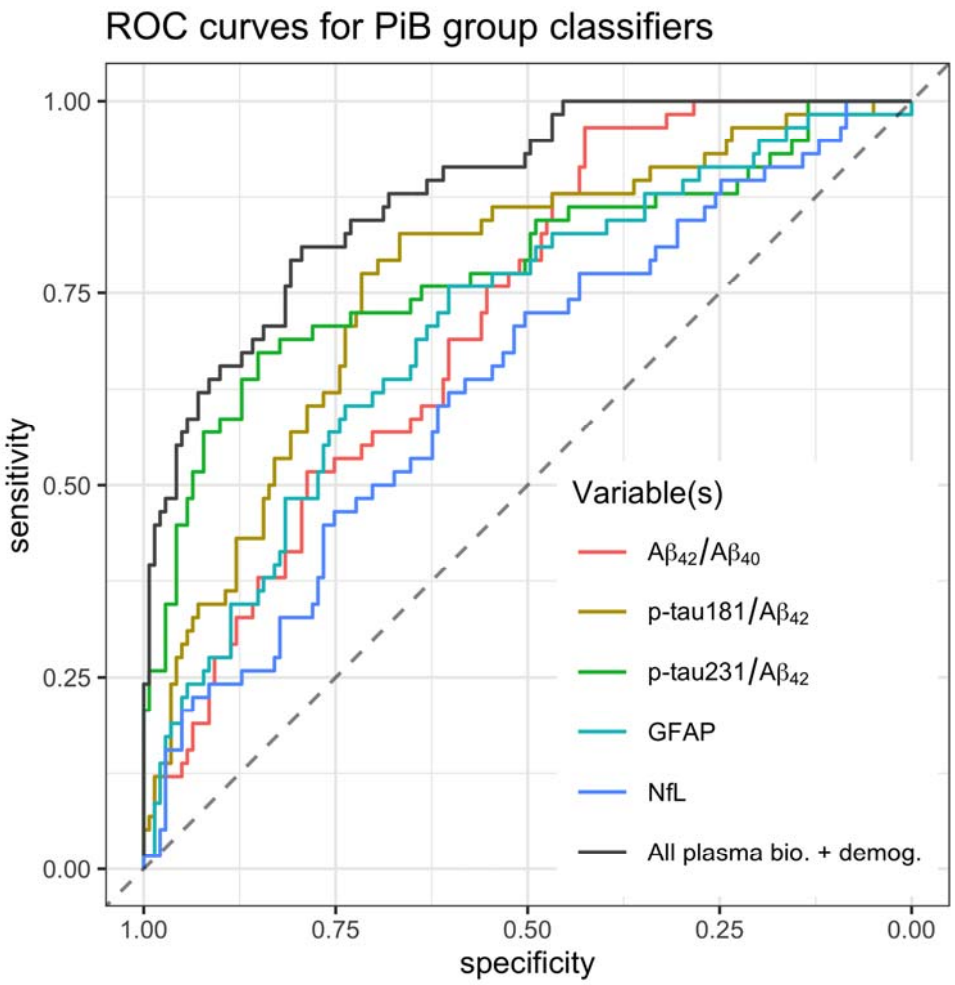

Figure 1: Receiver operating characteristic curves for univariate classifiers and the best multivariate classifier (including all plasma measures, age, sex, race, and APOE e4 status as features) for predicting PiB group. APOE, apolipoprotein E; bio., biomarkers; demog., demographics; GFAP, glial fibrillary acidic protein; NfL, neurofilament light chain; PiB, Pittsburgh compound B; p-tau, phosphorylated tau; ROC, receiver operating characteristic.

3.2.2 Multivariable models

Classifiers based on multiple predictors had slightly better performance than classifiers based on single predictors. The classifier with the highest AUC in 10-fold cross-validation

was a gradient boosting machine, yielding an AUC = 0.88 (95% CI = [0.73, 0.89]). The ROC curve for this classifier is shown in Figure 1. At the operating point with the highest balanced accuracy, this classifier achieved 79% specificity and 81% sensitivity.

Variable importances for the top 10 classifiers are shown in Supplementary Figure 8. p-tau231 was consistently the most important variable in these models, followed by $A\beta_{42}/A\beta_{40}$, p-tau231/$A\beta_{42}$, and p-tau181/$A\beta_{42}$.

3.3 Longitudinal intraclass correlation coefficients

Longitudinal ICCs over a median follow-up period of 6.1 years (IQR: 4, 8.6) are presented in Table 2 and Supplementary Table 2. Plasma measures had lower longitudinal ICC than that of cDVR in the whole sample and among PiB+ individuals.

Table 2: *Longitudinal intraclass correlation coefficients (ICCs).*

Biomarker	Overall		PiB−		PiB+	
	ICC	95% CI	ICC	95% CI	ICC	95% CI
$A\beta_{42}/A\beta_{40}$	0.66	(0.6–0.72)	0.67	(0.57–0.75)	0.68	(0.56–0.78)
p-tau181/$A\beta_{42}$	0.67	(0.59–0.73)	0.61	(0.5–0.7)	0.62	(0.47–0.73)
p-tau231/$A\beta_{42}$	0.75	(0.69–0.8)	0.57	(0.46–0.66)	0.75	(0.63–0.83)
GFAP	0.78	(0.72–0.82)	0.79	(0.73–0.84)	0.77	(0.67–0.85)
NfL	0.67	(0.6–0.72)	0.72	(0.64–0.79)	0.63	(0.48–0.74)
PiB cDVR	0.96	(0.94–0.97)	0.70	(0.62–0.77)	0.96	(0.94–0.98)

Abbreviations: Aβ, amyloid-β; cDVR, cortical distribution volume ratio; CI, confidence interval; GFAP, glial fibrillary acidic protein; ICC, intraclass correlation coefficient; NfL, neurofilament light chain; PiB, Pittsburgh compound B; p-tau, phosphorylated tau.

3.4 Longitudinal plasma biomarker trajectories by brain amyloid status

At the index visit, PiB+ individuals had lower $A\beta_{42}/A\beta_{40}$ ($\beta = -7.58 \times 10^{-3}$, SE = 1.41×10^{-3}, $p = 2.36 \times 10^{-7}$) and higher p-tau181/$A\beta_{42}$ ($\beta = 0.599$, SE = 0.129, $p = 6.16 \times 10^{-6}$), p-tau231/$A\beta_{42}$ ($\beta = 1.86$, SE = 0.243, $p = 1.28 \times 10^{-12}$), and GFAP ($\beta = 44.1$, SE = 11.6, $p = 1.81 \times 10^{-4}$) in adjusted models (Figure 2 and Supplementary Table 3). Longitudinal change in $A\beta_{42}/A\beta_{40}$ was not statistically significant among PiB+ individuals while PiB− individuals exhibited decreases ($\beta = -3.85 \times 10^{-4}$, SE = 9.77×10^{-5}, $p = 1.96 \times 10^{-4}$) (Supplementary Table 4). On the other hand, PiB+ individuals exhibited increases in p-tau181/$A\beta_{42}$ ($\beta = 6.53 \times 10^{-2}$, SE = 2.80×10^{-2}, $p = 2.11 \times 10^{-2}$) and p-tau231/$A\beta_{42}$ ($\beta = 0.110$, SE = 4.39×10^{-2}, $p = 1.41 \times 10^{-2}$), whereas the change in these ratios was not statistically significant among PiB− individuals. Both PiB groups exhibited longitudinal increases in NfL and GFAP, and their rates of change did not differ by PiB group in adjusted models.

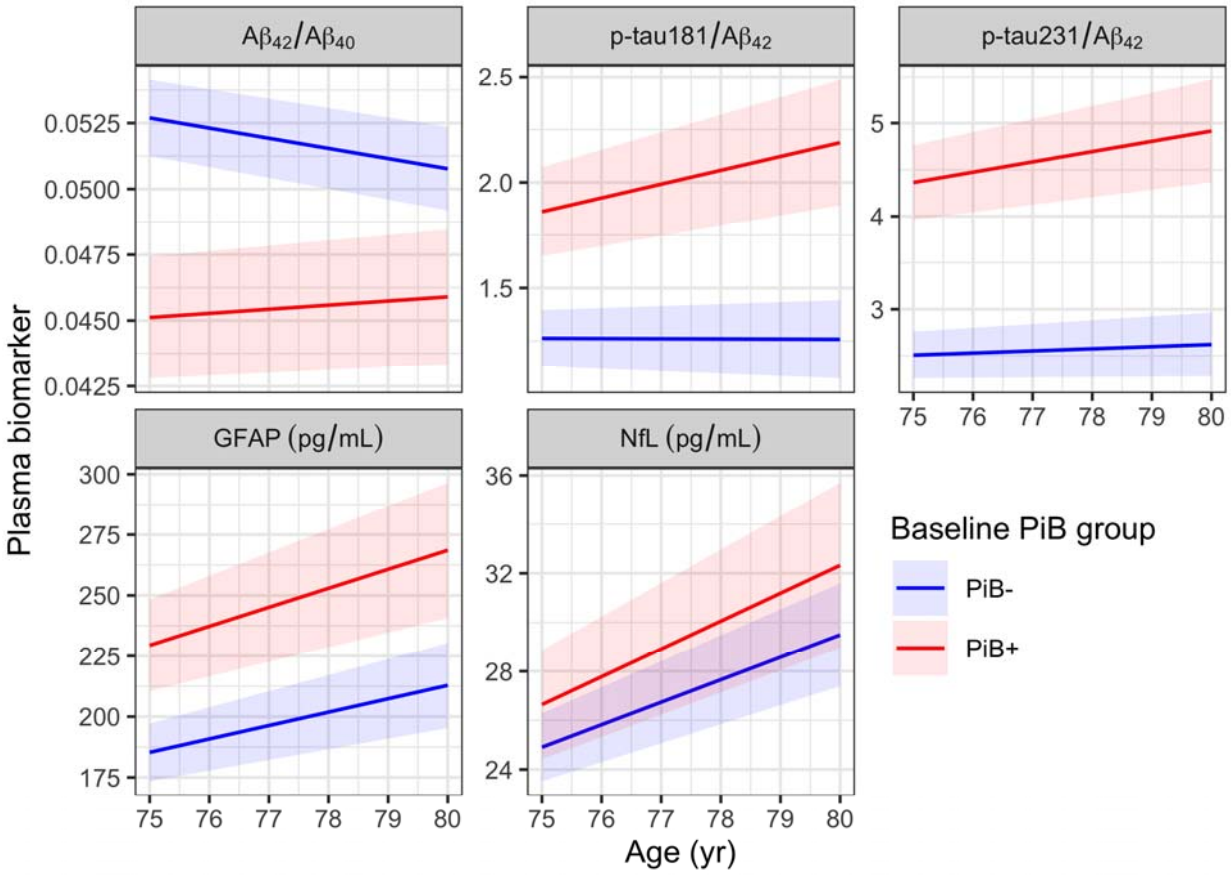

Figure 2: Plasma biomarker trajectories estimated using linear mixed effects models. Bands indicate 95% confidence intervals. GFAP, glial fibrillary acidic protein; NfL, neurofilament light chain; PiB, Pittsburgh compound B; p-tau, phosphorylated tau.

3.5 Associations among longitudinal rates of change in plasma biomarkers and brain amyloid

Based on our findings that the ratios $A\beta_{42}/A\beta_{40}$, p-tau181/$A\beta_{42}$ and p-tau231/$A\beta_{42}$ had higher AUCs for classifying individuals by PiB status and higher longitudinal ICCs than the individual measures that made up the ratios, we did not include the individual plasma measures $A\beta_{40}$, $A\beta_{42}$, p-tau181, or p-tau231 in the remaining analyses.

The correlation between longitudinal rates of change in p-tau181/$A\beta_{42}$ and p-tau231/$A\beta_{42}$ was high and statistically significant (r = 0.87, 95% CI = [0.62, 0.96]) (Supplementary Figure 10). We additionally found statistically significant correlations between the rates of change in GFAP and NfL (r = 0.88 [0.63, 0.97]), GFAP and cDVR (r = 0.5, 95% CI = [0.26, 0.68]), and NfL and cDVR (r = 0.4 [0.13, 0.62]). There was a trend toward a positive correlation between cDVR and the two p-tau ratios (r = 0.28 [-0.02, 0.53] for p-tau181/ $A\beta_{42}$ and r = 0.27 [-0.07, 0.56] for p-tau231/$A\beta_{42}$), and a negative correlation between $A\beta_{42}/A\beta_{40}$ and GFAP (r = -0.56 [-0.87, 0.07]).

3.6 Temporal order of changes in plasma biomarkers and brain amyloid

Estimated PS and biomarker trajectories, along with the observed biomarker data, are shown in Figure 3. Consistent with expectation, both PS and the subject-specific time-shift parameter at last visit were higher among individuals with MCI or dementia compared to cognitively normal individuals (Wilcoxon rank-sum test $p = 4.51 \times 10^{-6}$ for PS, $p = 0.0032$ for time-shift variable τ).

To understand the relative order of biomarker changes, we computed percent relative change by dividing the derivative in PS of the estimated trajectory by the trajectory itself for each biomarker (Figure 4 and Supplementary Figure 11) and examined where the peak percent relative change occurs relative to the PS value corresponding to the PiB+ threshold. This analysis suggested that the earliest change occurs in $A\beta_{42}/A\beta_{40}$. Peak relative decline in $A\beta_{42}/A\beta_{40}$ (-1% per year) preceded brain amyloid positivity onset by 41 years (95% CI = [32, 53]) (Supplementary Table 5). Time intervals between brain amyloid positivity onset and peak relative change in the remaining plasma biomarkers were not statistically significant.

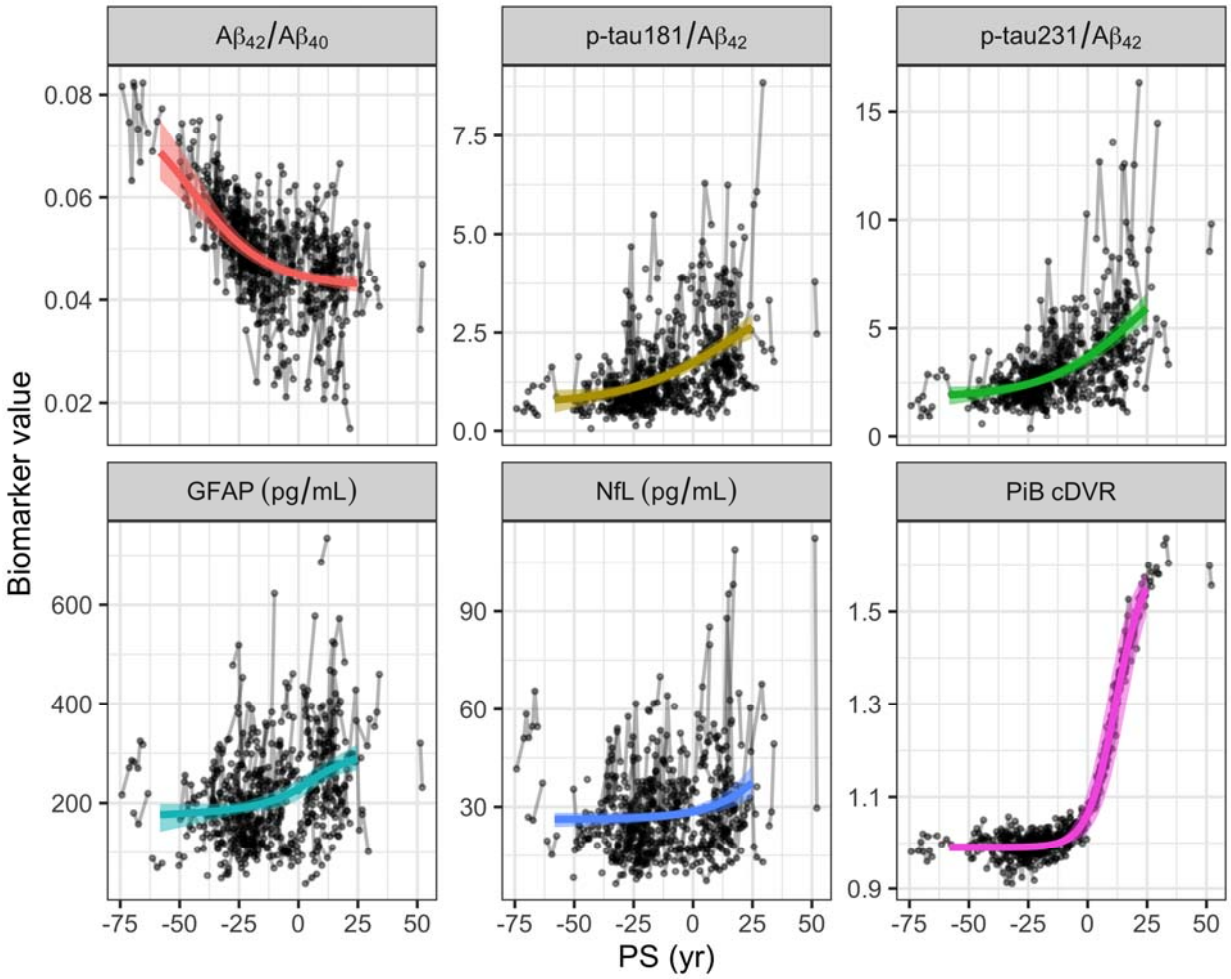

Figure 3: Biomarker trajectories estimated after alignment of individual-level longitudinal data using the progression score (PS) model. Bands indicate the 95% confidence intervals for the trajectory estimates. PS scale was calibrated after model fitting such that at PS = 0, the estimated trajectory for PiB cDVR attains the value 1.06, which is the PiB positivity threshold. Since PS is time-shifted age, it is in the units of years. cDVR, cortical distribution volume ratio; GFAP, glial fibrillary acidic protein; NfL, neurofilament light chain; PiB, Pittsburgh compound B; PS, progression score; p-tau, phosphorylated tau.

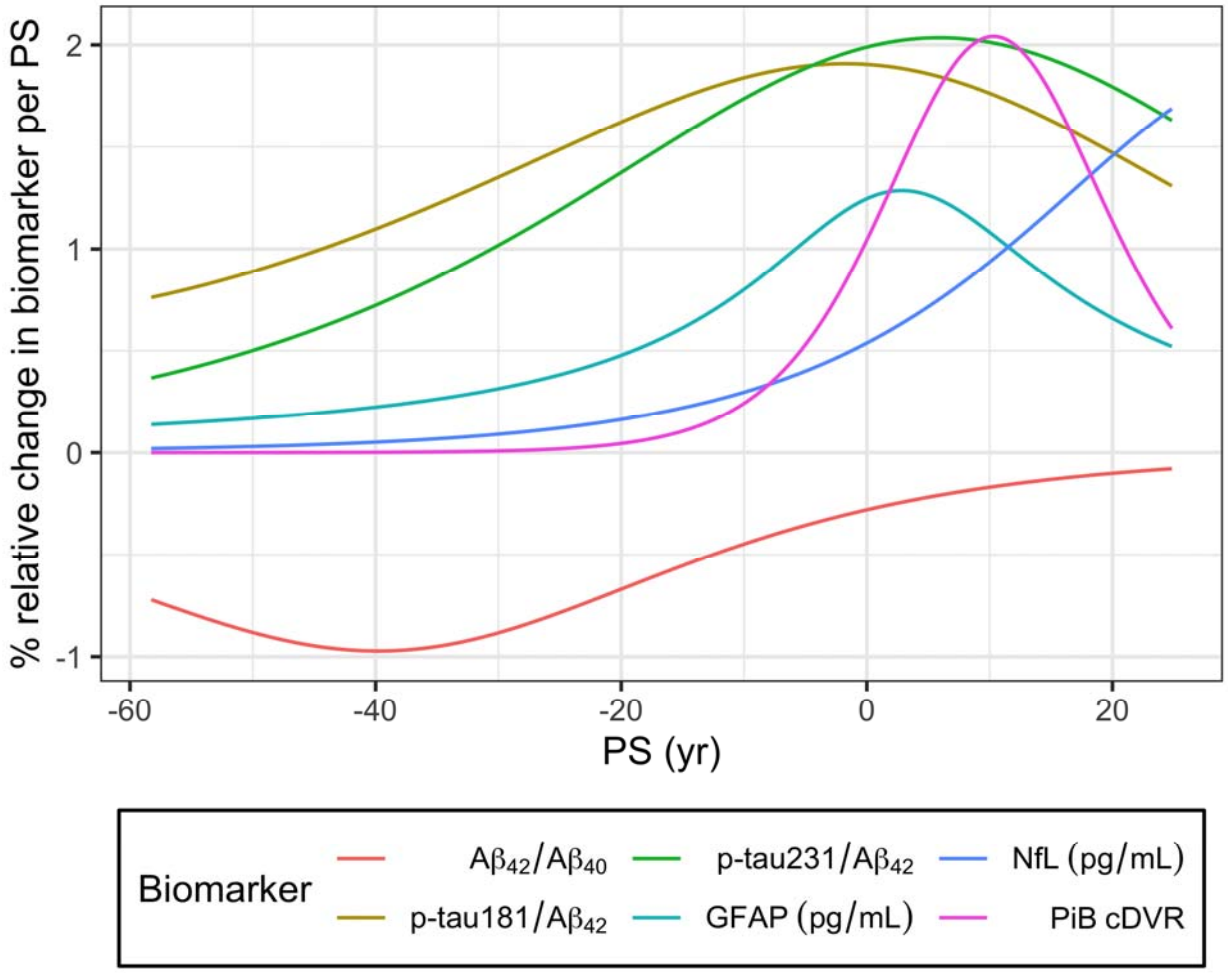

Figure 4: Percent relative change in biomarkers per progression score (PS) as a function of PS. cDVR, cortical distribution volume ratio; GFAP, glial fibrillary acidic protein; NfL, neurofilament light chain; PiB, Pittsburgh compound B; PS, progression score; p-tau, phosphorylated tau.

4 Discussion

This study focused on longitudinal changes in plasma biomarkers of AD neuropathology and neurodegeneration relative to amyloid plaques, the emergence of which marks the beginning of preclinical AD. We first replicated prior findings of the extent to which plasma biomarkers predict PET brain amyloid status. In our sample of cognitively normal individuals, the plasma measures with the best amyloid PET status classification performance were the p-tau to $A\beta_{42}$ ratios. Our $A\beta_{42}/A\beta_{40}$ AUC is consistent with the AUC reported in other studies of cognitively normal individuals based on Simoa immunoassays [15,33]. Our findings also corroborate previous studies indicating that plasma p-tau measures more closely reflect brain amyloid levels compared to plasma measures of amyloid [16] and that p-tau231 has the highest AUC at the preclinical stage [14–16]. As expected, based on our univariate results, plasma p-tau, specifically p-tau231, and Aβ measures were the most important variables in the best multivariate classifier, which outperformed univariate classifiers and had a sensitivity and specificity of about 80% at its optimal operating point.

The main contribution of our paper is the longitudinal examination of changes in plasma biomarkers. Longitudinal reliability, as measured by ICC, of plasma measures was lower than that of the brain amyloid PET measure in the whole sample and among PiB+, but comparable among PiB−. We found a statistically significant longitudinal decrease in plasma $A\beta_{42}/A\beta_{40}$ among PiB− individuals, whereas longitudinal change among PiB+ individuals was not statistically significant. This, along with the finding that PiB+ individuals have lower $A\beta_{42}/A\beta_{40}$ at index visit compared to PiB−, suggests that plasma

$A\beta_{42}/A\beta_{40}$ declines prior to the emergence of elevated levels of brain amyloid and then may reach a plateau. Based on the estimated cross-sectional PiB group difference and the rate of decline among PiB− individuals, the decline in plasma $A\beta_{42}/A\beta_{40}$ would be expected to span at least 20 years prior to brain amyloid positivity. Other studies have also found that amyloid PET is elevated or increases only when plasma $A\beta_{42}/A\beta_{40}$ is low [34,35].

In bivariate LMEMs, the plasma measures that most closely changed in conjunction with brain amyloid levels were GFAP and NfL. Rates of change in p-tau181/$A\beta_{42}$ and p-tau231/$A\beta_{42}$ also aligned with rate of change in brain amyloid level, but these associations were not statistically significant. Plasma $A\beta_{42}/A\beta_{40}$ did not exhibit a statistically significant longitudinal correlation with brain amyloid or any other plasma biomarker, but had a trend-level negative association with GFAP. This difference in the longitudinal correlations for brain amyloid and plasma amyloid is likely due to the different time windows in which these two measures are dynamic, with plasma amyloid exhibiting changes decades prior to brain amyloid. Rates of change were highly correlated between p-tau181/$A\beta_{42}$ and p-tau231/$A\beta_{42}$, and between GFAP and NfL. Our findings agree with the plasma biomarker findings from the TRAILBLAZER-ALZ clinical trial, where longitudinal change in brain amyloid was correlated with change in plasma GFAP but not $A\beta_{42}/A\beta_{40}$ [36].

Our progression score model result suggests that $A\beta_{42}/A\beta_{40}$ may decline over several decades leading up to the onset of brain amyloid accumulation. However, these changes in plasma $A\beta_{42}/A\beta_{40}$ are subtle, with relative change peaking at -1% per year. Brain PET measures fibrillar amyloid, an advanced stage in the amyloid aggregation process, whereas

plasma biomarkers reflect earlier forms such as diffuse amyloid pathology. This difference is one possible explanation of the timing difference between plasma and brain amyloid measures. These results highlight plasma $A\beta_{42}/A\beta_{40}$ as a potential marker for detecting early changes prior to the emergence of brain amyloid plaques, but it remains unclear whether such small differences can be reliably detected at the individual level. Given that this plasma measure may plateau by the time one has high levels of brain amyloid, its utility in a longitudinal context among amyloid PET positive individuals would likely be limited. Other plasma biomarkers we investigated exhibited more pronounced changes over time, with p-tau ratios exhibiting relative changes around 2% per year, and these changes occurred closer in time to brain amyloid accumulation. This finding is consistent with literature demonstrating that plasma p-tau measurements better align with brain amyloid rather than tau levels as measured with PET [37,38]. Our results regarding longitudinal changes and temporal order are consistent with other studies that investigated longitudinal plasma measurements [10–12]. More extensive longitudinal data will allow examination of temporal order variation at the individual level.

Our study has several limitations. It is possible that we were unable to detect a statistically significant PiB group difference in the longitudinal rates of change in p-tau, GFAP, and NfL due to the limited number of participants included in our study. We used a time-invariant residual correlation structure in our progression score model, which is easier to estimate than a time-varying correlation structure, but may be less appropriate. The characterization of biomarker trajectories was informed mainly by data from cognitively normal individuals, and the lack of data from late dementia stages prevented us from describing the full extent of the natural history of these biomarkers. The longitudinal

follow-up duration was much shorter than the estimated time intervals over which plasma biomarkers change, preventing us from verifying our estimates using individual-level data.

Our study also has important strengths. The median follow-up duration for our plasma measures, 6.1 years, is higher than the follow-up duration of 2–4 years in existing longitudinal plasma biomarker studies [8–13]. We used advanced multivariable classifiers and employed cross-validation to calculate ROCs and classification performance metrics to prevent overestimating classifier performance. When investigating associations among rates of longitudinal change, instead of calculating slopes and then correlating them, we employed bivariate LMEMs. While the former approach treats slopes as observed parameters and therefore, does not accurately incorporate the error in their estimation, the bivariate LMEM considers slopes as random variables and as a result, factors in the uncertainty in the slopes.

In conclusion, our results corroborate that p-tau231 as a superior biomarker of amyloid burden in preclinical disease but suggest that plasma $A\beta_{42}/A\beta_{40}$ is dynamic prior to brain amyloid accumulation. Other plasma measures, GFAP in particular, may more closely align with longitudinal change in brain amyloid accumulation. Plasma biomarkers are promising tools for detecting and monitoring longitudinal change along the disease spectrum and can be useful for identifying candidates for a brain amyloid PET scan. Given the emerging anti-amyloid therapies, being able to assess brain amyloid levels using easy and low cost measures such as plasma biomarkers will be particularly useful and important.

5 Acknowledgments

This study was supported by the Intramural Research Program of the National Institute on Aging, National Institutes of Health. KB is supported by the Swedish Research Council (#2017-00915), the Alzheimer Drug Discovery Foundation (ADDF), USA (#RDAPB-201809-2016615), the Swedish Alzheimer Foundation (#AF-742881), Hjärnfonden, Sweden (#FO2017-0243), the Swedish state under the agreement between the Swedish government and the County Councils, the ALF-agreement (#ALFGBG-715986), the European Union Joint Program for Neurodegenerative Disorders (JPND2019-466-236), and the National Institute of Health (NIH), USA, (grant #1R01AG068398-01). HZ is a Wallenberg Scholar supported by grants from the Swedish Research Council (#2022-01018), the European Union's Horizon Europe research and innovation programme under grant agreement No 101053962, Swedish State Support for Clinical Research (#ALFGBG-71320), the Alzheimer Drug Discovery Foundation (ADDF), USA (#201809-2016862), the AD Strategic Fund and the Alzheimer's Association (#ADSF-21-831376-C, #ADSF-21-831381-C, and #ADSF-21-831377-C), the Bluefield Project, the Olav Thon Foundation, the Erling-Persson Family Foundation, Stiftelsen för Gamla Tjänarinnor, Hjärnfonden, Sweden (#FO2022-0270), the European Union's Horizon 2020 research and innovation programme under the Marie Skłodowska-Curie grant agreement No 860197 (MIRIADE), the European Union Joint Programme – Neurodegenerative Disease Research (JPND2021-00694), and the UK Dementia Research Institute at UCL (UKDRI-1003). BMJ was partially funded by NIH NIA R01 AG027161.

6 References

1. Jack CR, Bennett DA, Blennow K, et al. NIA-AA research framework: Toward a biological definition of Alzheimer's disease. *Alzheimer's & Dementia*. 2018;14(4):535-562. doi:10.1016/j.jalz.2018.02.018

2. Hansson O, Edelmayer RM, Boxer AL, et al. The Alzheimer's Association appropriate use recommendations for blood biomarkers in Alzheimer's disease. *Alzheimer's & Dementia*. 2022;(June):1-18. doi:10.1002/alz.12756

3. Schindler SE, Bollinger JG, Ovod V, et al. High-precision plasma β-amyloid 42/40 predicts current and future brain amyloidosis. *Neurology*. 2019;93(17):e1647-e1659. doi:10.1212/WNL.0000000000008081

4. Tosun D, Veitch D, Aisen P, et al. Detection of β-amyloid positivity in Alzheimer's Disease Neuroimaging Initiative participants with demographics, cognition, MRI and plasma biomarkers. *Brain Communications*. 2021;3(2). doi:10.1093/braincomms/fcab008

5. Cianflone A, Coppola L, Mirabelli P, Salvatore M. Predictive accuracy of blood-derived biomarkers for amyloid-β brain deposition along with the Alzheimer's disease continuum: A systematic review. Hall A, ed. *Journal of Alzheimer's Disease*. 2021;84(1):393-407. doi:10.3233/JAD-210496

6. Ashford MT, Veitch DP, Neuhaus J, Nosheny RL, Tosun D, Weiner MW. The search for a convenient procedure to detect one of the earliest signs of Alzheimer's disease: A systematic review of the prediction of brain amyloid status. *Alzheimer's & Dementia*. 2021;17(5):866-887. doi:10.1002/alz.12253

7. Benedet AL, Brum WS, Hansson O, et al. The accuracy and robustness of plasma biomarker models for amyloid PET positivity. *Alzheimer's Research & Therapy*. 2022;14(1):1-11. doi:10.1186/s13195-021-00942-0

8. Chatterjee P, Pedrini S, Doecke JD, et al. Plasma Aβ42/40 ratio, p-tau181, GFAP, and NfL across the Alzheimer's disease continuum: A cross-sectional and longitudinal study in the AIBL cohort. *Alzheimer's & Dementia*. 2022;(February):1-18. doi:10.1002/alz.12724

9. O'Connor A, Karikari TK, Poole T, et al. Plasma phospho-tau181 in presymptomatic and symptomatic familial Alzheimer's disease: a longitudinal cohort study. *Molecular Psychiatry*. 2021;26(10):5967-5976. doi:10.1038/s41380-020-0838-x

10. Burnham SC, Fandos N, Fowler C, et al. Longitudinal evaluation of the natural history of amyloid-β in plasma and brain. *Brain Communications*. 2020;2(1):1-7. doi:10.1093/braincomms/fcaa041

11. Moscoso A, Grothe MJ, Ashton NJ, et al. Time course of phosphorylated-tau181 in blood across the Alzheimer's disease spectrum. *Brain*. 2021;144(1):325-339. doi:10.1093/brain/awaa399

12. Chen TB, Lai YH, Ke TL, et al. Changes in plasma amyloid and tau in a longitudinal study of normal aging, mild cognitive impairment, and Alzheimer's disease. *Dementia and Geriatric Cognitive Disorders*. 2020;48(3-4):180-195. doi:10.1159/000505435

13. Rauchmann BS, Schneider-Axmann T, Perneczky R. Associations of longitudinal plasma p-tau181 and NfL with tau-PET, Aβ-PET and cognition. *Journal of Neurology, Neurosurgery and Psychiatry*. 2021;92(12):1289-1295. doi:10.1136/jnnp-2020-325537

14. Ashton NJ, Janelidze S, Mattsson-Carlgren N, et al. Differential roles of aβ42/40, p-tau231 and p-tau217 for alzheimer's trial selection and disease monitoring. *Nature Medicine*. 2022;28(12):2555-2562. doi:10.1038/s41591-022-02074-w

15. Milà-Alomà M, Ashton NJ, Shekari M, et al. Plasma p-tau231 and p-tau217 as state markers of amyloid-β pathology in preclinical alzheimer's disease. *Nature Medicine*. 2022;28(9):1797-1801. doi:10.1038/s41591-022-01925-w

16. Meyer PF, Ashton NJ, Karikari TK, et al. Plasma p-tau231, p-tau181, PET biomarkers, and cognitive change in older adults. *Annals of Neurology*. 2022;91(4):548-560. doi:10.1002/ana.26308

17. Fuld PA. Psychological testing in the differential diagnosis of the dementias. In: Katzman R, Terry RD, Bick KL, eds. *Alzheimer's Disease: Senile Dementia and Related Disorders*. Raven Press; 1978:185-193.

18. Morris JC. The clinical dementia rating (CDR). *Neurology*. 1993;43(11):2412.2-2412-a. doi:10.1212/WNL.43.11.2412-a

19. Petersen RC. Mild cognitive impairment as a diagnostic entity. *Journal of Internal Medicine*. 2004;256(3):183-194. doi:10.1111/j.1365-2796.2004.01388.x

20. Association AP. *Diagnostic and Statistical Manual of Mental Disorders: DSM-III-R*. 3rd ed. re. American Psychiatric Association; 1987.

21. Zhou Y, Resnick SM, Ye W, et al. Using a reference tissue model with spatial constraint to quantify [11C] Pittsburgh compound B PET for early diagnosis of Alzheimer's disease. *NeuroImage*. 2007;36(2):298-312. doi:10.1016/j.neuroimage.2007.03.004

22. Bilgel M, Beason-Held L, An Y, Zhou Y, Wong DF, Resnick SM. Longitudinal evaluation of surrogates of regional cerebral blood flow computed from dynamic amyloid PET imaging. *Journal of Cerebral Blood Flow & Metabolism*. 2020;40(2):288-297. doi:10.1177/0271678X19830537

23. Bilgel M, Wong DF, Moghekar AR, Ferrucci L, Resnick SM. Causal links among amyloid, tau, and neurodegeneration. *Brain Communications*. 2022;4(4):2021.07.01.21259866. doi:10.1093/braincomms/fcac193

24. Peng Z, Duggan MR, Dark HE, et al. Association of liver disease with brain volume loss, cognitive decline, and plasma neurodegenerative disease biomarkers. *Neurobiology of Aging*. 2022;120:34-42. doi:10.1016/j.neurobiolaging.2022.08.004

25. Karikari TK, Pascoal TA, Ashton NJ, et al. Blood phosphorylated tau 181 as a biomarker for Alzheimer's disease: a diagnostic performance and prediction modelling study using data from four prospective cohorts. *The Lancet Neurology*. 2020;19(5):422-433. doi:10.1016/S1474-4422(20)30071-5

26. Ashton NJ, Pascoal TA, Karikari TK, et al. Plasma p-tau231: A new biomarker for incipient Alzheimer's disease pathology. *Acta Neuropathologica*. 2021;141(5):709-724. doi:10.1007/s00401-021-02275-6

27. LeDell E, Poirier S. H2O AutoML: Scalable Automatic Machine Learning. *7th ICML Workshop on Automated Machine Learning (AutoML)*. Published online 2020. https://www.automl.org/wp-content/uploads/2020/07/AutoML{_}2020{_}paper{_}61.pdf

28. LeDell E, Gill N, Aiello S, et al. *H2o: R Interface for the H2o Scalable Machine Learning Platform*.; 2022. https://github.com/h2oai/h2o-3

29. R Core Team. *R: A Language and Environment for Statistical Computing*. R Foundation for Statistical Computing; 2020. https://www.R-project.org/

30. Binette AP, Janelidze S, Cullen N, et al. Confounding factors of Alzheimer's disease plasma biomarkers and their impact on clinical performance. *Alzheimer's & Dementia*. Published online September 2022. doi:10.1002/alz.12787

31. Pinheiro J, Bates D, R-core. *Nlme: Linear and Nonlinear Mixed Effects Models*.; 2021. https://svn.r-project.org/R-packages/trunk/nlme/

32. Bilgel M, Jedynak BM. Predicting time to dementia using a quantitative template of disease progression. *Alzheimer's & Dementia: Diagnosis, Assessment & Disease Monitoring*. 2019;11(1):205-215. doi:10.1016/j.dadm.2019.01.005

33. Vergallo A, Mégret L, Lista S, et al. Plasma amyloid β 40/42 ratio predicts cerebral amyloidosis in cognitively normal individuals at risk for Alzheimer's disease. *Alzheimer's & Dementia*. 2019;15(6):764-775. doi:10.1016/j.jalz.2019.03.009

34. Rembach A, Faux NG, Watt AD, et al. Changes in plasma amyloid beta in a longitudinal study of aging and Alzheimer's disease. *Alzheimer's & Dementia*. 2014;10(1):53-61. doi:10.1016/j.jalz.2012.12.006

35. Pereira JB, Janelidze S, Stomrud E, et al. Plasma markers predict changes in amyloid, tau, atrophy and cognition in non-demented subjects. *Brain*. 2021;144(9):2826-2836. doi:10.1093/brain/awab163

36. Pontecorvo MJ, Lu M, Burnham SC, et al. Association of donanemab treatment with exploratory plasma biomarkers in early symptomatic Alzheimer disease. *JAMA Neurology*. 2022;79(12):1250. doi:10.1001/jamaneurol.2022.3392

37. Mattsson-Carlgren N, Andersson E, Janelidze S, et al. Aβ deposition is associated with increases in soluble and phosphorylated tau that precede a positive tau pet in Alzheimer's disease. *Science Advances*. 2020;6(16). doi:10.1126/sciadv.aaz2387

38. Therriault J, Vermeiren M, Servaes S, et al. Association of phosphorylated tau biomarkers with amyloid positron emission tomography vs tau positron emission tomography. *JAMA Neurology*. 2022;In press. doi:10.1001/jamaneurol.2022.4485

39. Bilgel M, An Y, Zhou Y, et al. Individual estimates of age at detectable amyloid onset for risk factor assessment. *Alzheimer's & Dementia*. 2016;12(4):373-379. doi:10.1016/j.jalz.2015.08.166

40. Stan Development Team. RStan: The R interface to Stan. Published online 2020. http://mc-stan.org/

Supplementary Material

Sample inclusion and exclusion criteria

Of the 229 Baltimore Longitudinal Study of Aging (BLSA) participants with amyloid PET scans prior to March 13, 2020, one was excluded due to a previously unreported myocardial infarction prior to enrollment (an exclusion criterion), four were excluded due to insufficient or inadequate PET data that prevented image processing, and three were excluded due to missing apolipoprotein E (*APOE*) genotyping. Of the remaining 221 participants, 199 had at least one visit with measurements for the full set of plasma biomarkers. Data from these 199 participants comprised the current cross-sectional and longitudinal datasets.

The index visit, defined as the earliest cognitively normal visit with a full set of plasma biomarker measurements, overlapped with an amyloid PET visit for all except two participants. For these two participants, the index visit was prior to their PET scans. We imputed their PiB group at the index visit (see below). The resulting cross-sectional dataset was used to examine the performance of plasma biomarkers in classifying individuals as PiB− or PiB+.

In longitudinal analyses, we included all plasma measures following the index visit as well as all plasma measures preceding the index visit if the (imputed) PiB group at the preceding visit was the same as the (imputed) PiB group at the index visit.

PiB group imputation

In the longitudinal PiB PET dataset for the participants included in this analysis, no individuals reverted from PiB+ to PiB−. All visits prior to a PiB− scan were assumed to be PiB−, and all visits following a PiB+ scan were assumed to be PiB+. Visits within one year of a PiB PET scan were imputed using the binary PiB group assigned to the PiB PET scan. Otherwise, for visits preceding a PiB+ scan, we used the participant's estimated amyloid onset age [39] to impute PiB group. If the visit occurred prior to estimated amyloid onset, it was imputed as PiB−. If the visit occurred more than 3 years following the estimated amyloid onset, it was imputed as PiB+. Otherwise, we did not impute PiB group.

6.1 Associations of plasma and PiB PET measures at index visit with eGFR, BMI, sex, and race

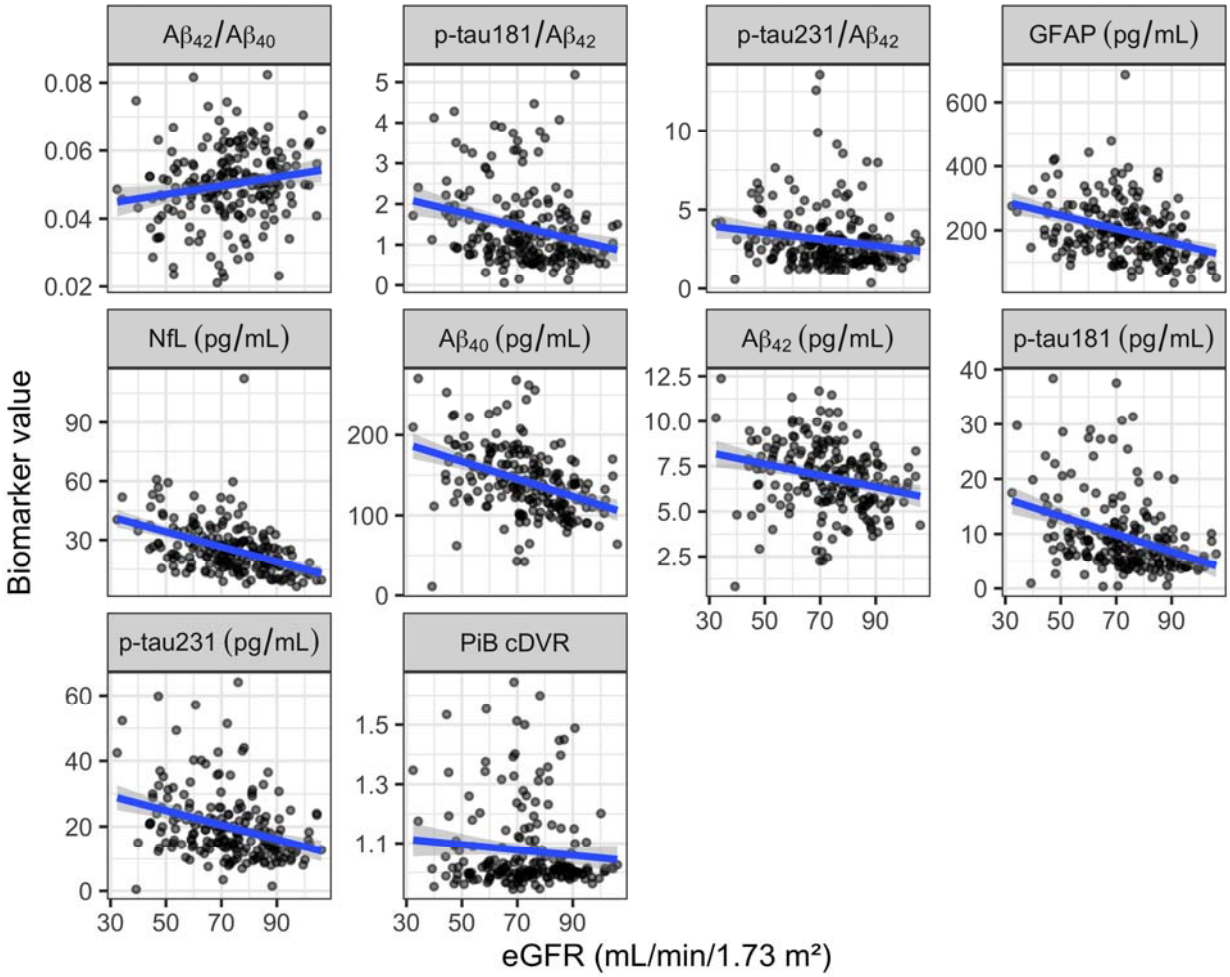

Supplementary Figure 1: Plasma and PiB PET measures at the index visit as a function of estimated glomerular filtration rate (eGFR). cDVR, cortical distribution volume ratio; GFAP, glial fibrillary acidic protein; NfL, neurofilament light chain; PiB, Pittsburgh compound B; p-tau, phosphorylated tau.

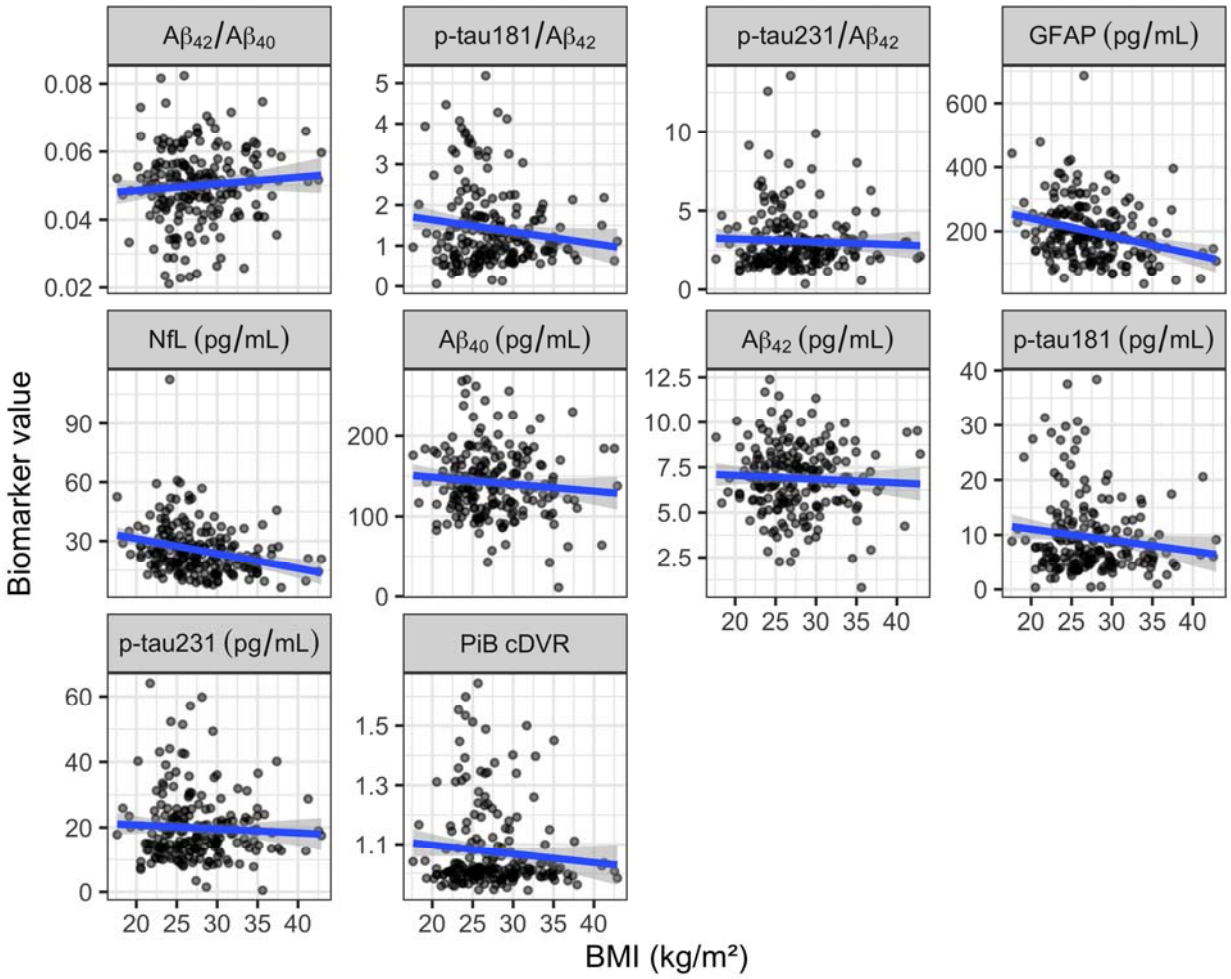

Supplementary Figure 2: Plasma and PiB PET measures at the index visit as a function of body mass index (BMI). cDVR, cortical distribution volume ratio; GFAP, glial fibrillary acidic protein; NfL, neurofilament light chain; PiB, Pittsburgh compound B; p-tau, phosphorylated tau.

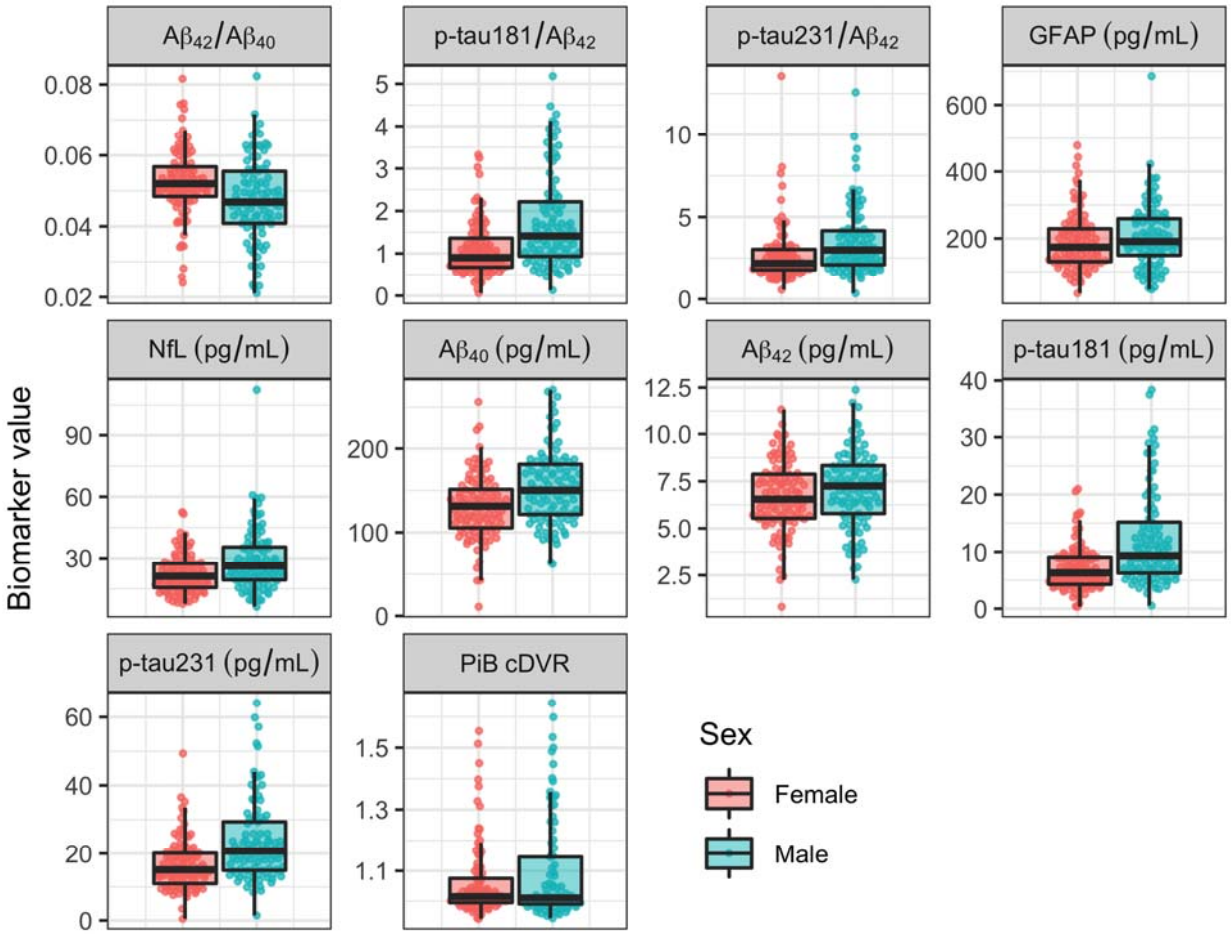

Supplementary Figure 3: Plasma and PiB PET measures at the index visit by sex and PiB group. cDVR, cortical distribution volume ratio; GFAP, glial fibrillary acidic protein; NfL, neurofilament light chain; PiB, Pittsburgh compound B; p-tau, phosphorylated tau.

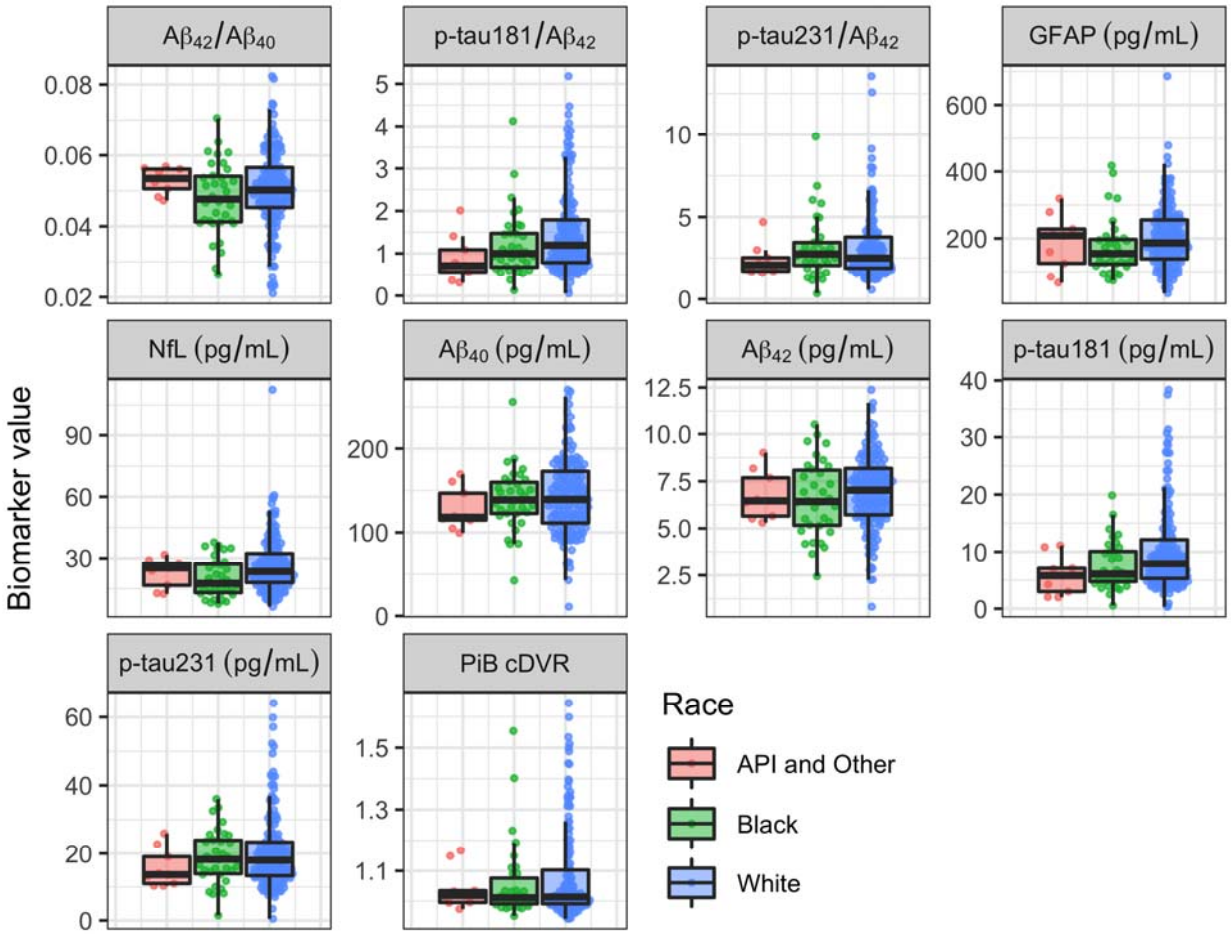

Supplementary Figure 4: Plasma and PiB PET measures at the index visit by race and PiB group. API, Asian/Pacific Islander; cDVR, cortical distribution volume ratio; GFAP, glial fibrillary acidic protein; NfL, neurofilament light chain; PiB, Pittsburgh compound B; p-tau, phosphorylated tau.

Correlations among plasma biomarkers and brain amyloid at index visit

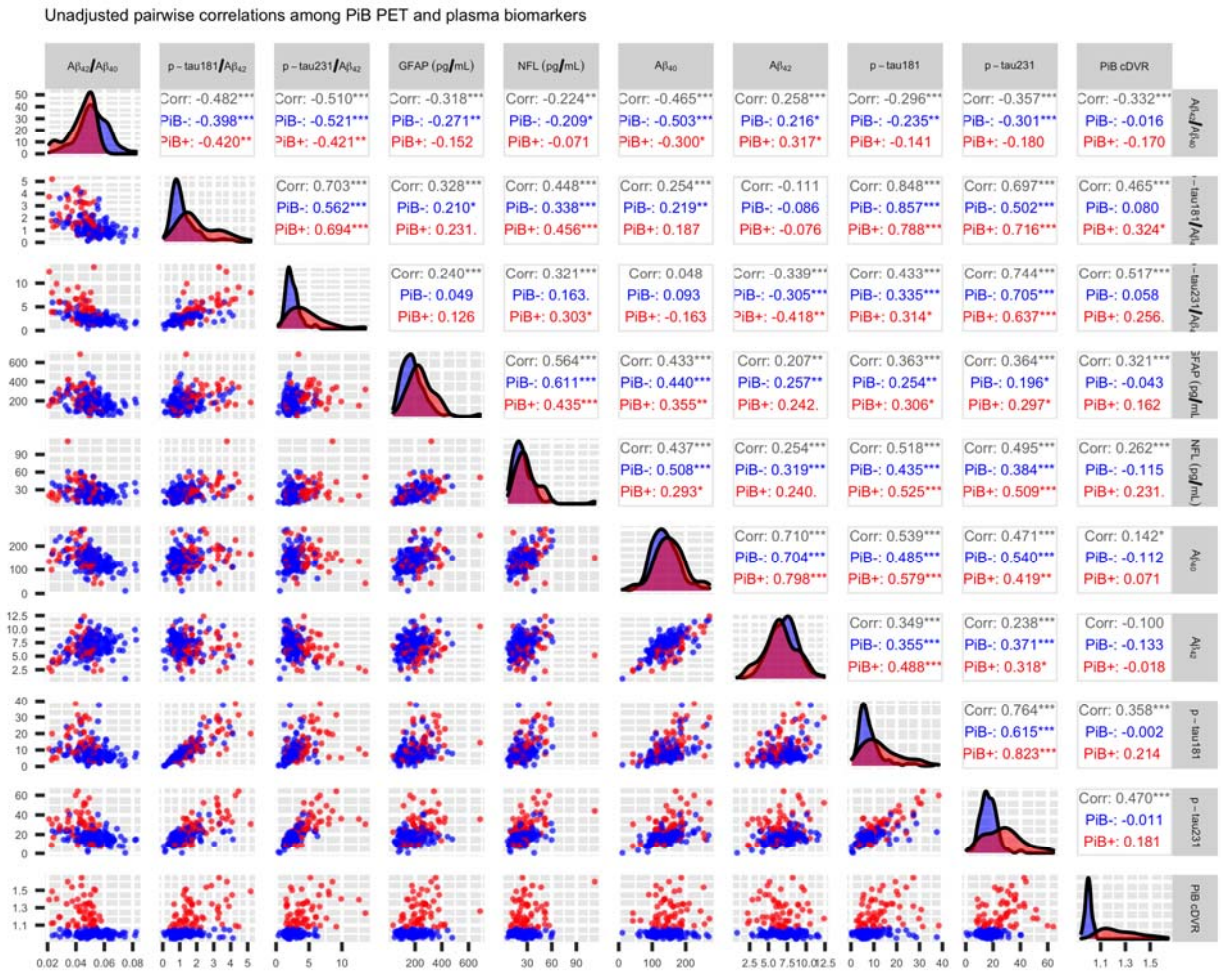

*Supplementary Figure 5: Cross-sectional pairwise correlations among plasma and PiB PET measures at the index visit. . p < .1, * p < .05, ** p < .01, *** p < .001. cDVR, cortical distribution volume ratio; GFAP, glial fibrillary acidic protein; NfL, neurofilament light chain; PiB, Pittsburgh compound B; p-tau, phosphorylated tau.*

Longitudinal plasma biomarker and PiB cDVR data used in analyses

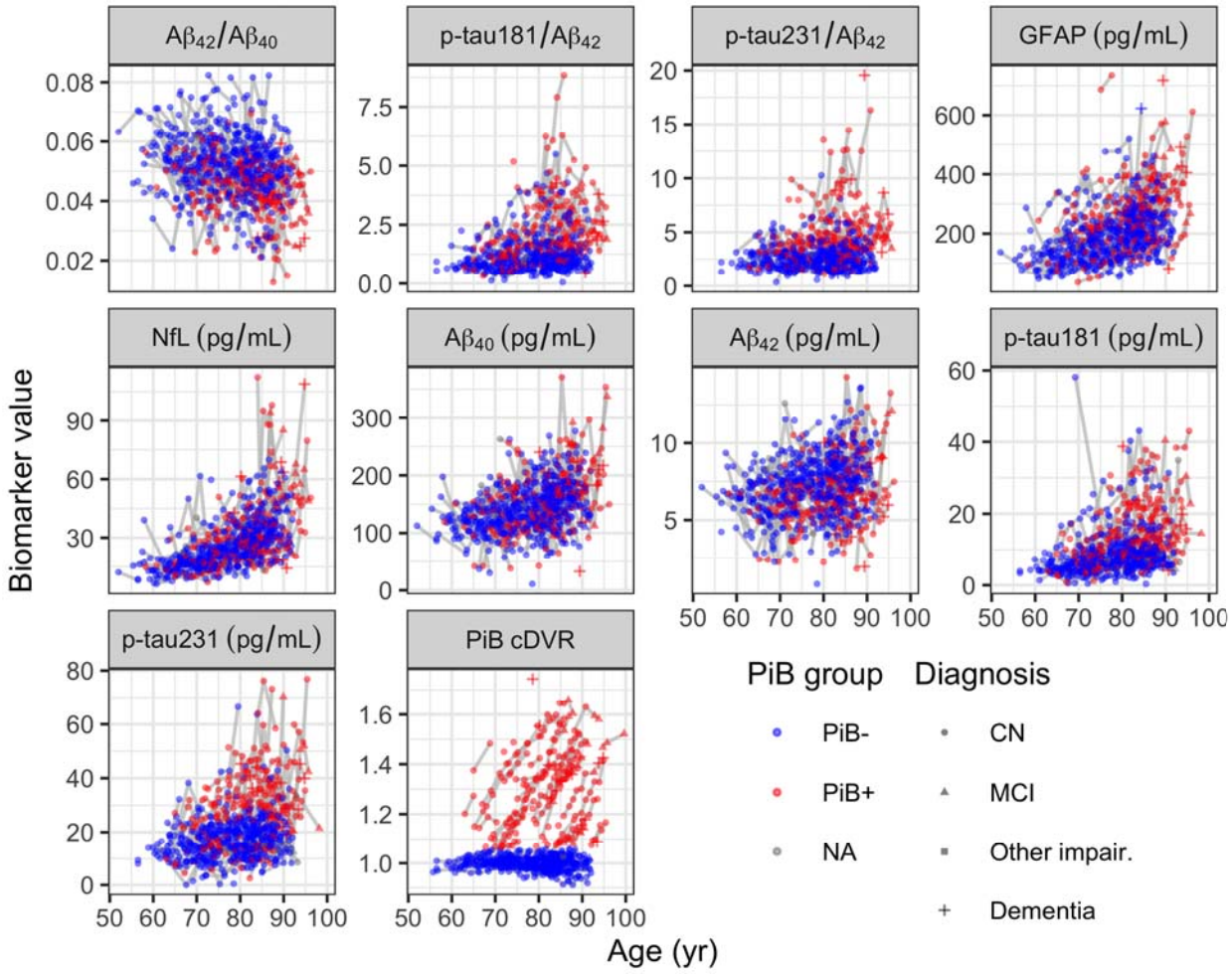

Supplementary Figure 6: Longitudinal plasma biomarkers and PiB cDVR versus age. cDVR, cortical distribution volume ratio; GFAP, glial fibrillary acidic protein; NfL, neurofilament light chain; PiB, Pittsburgh compound B; p-tau, phosphorylated tau.

Classification of brain amyloid status using plasma biomarkers

Supplementary Table 1: *AUCs for univariate models for predicting PiB group.*

Variable	AUC	95% CI
Age	0.63	(0.54–0.71)
$A\beta_{42}/A\beta_{40}$	0.72	(0.65–0.79)
p-tau181/$A\beta_{42}$	0.77	(0.7–0.84)
p-tau231/$A\beta_{42}$	0.78	(0.71–0.86)
GFAP	0.71	(0.63–0.79)
NfL	0.64	(0.55–0.72)
$A\beta_{40}$	0.62	(0.53–0.7)
$A\beta_{42}$	0.56	(0.47–0.65)
p-tau181	0.72	(0.63–0.8)
p-tau231	0.76	(0.67–0.85)

Abbreviations: Aβ, amyloid-β; AUC, area under the receiver operating characteristic curve; CI, confidence interval; GFAP, glial fibrillary acidic protein; NfL, neurofilament light chain; p-tau, phosphorylated tau.

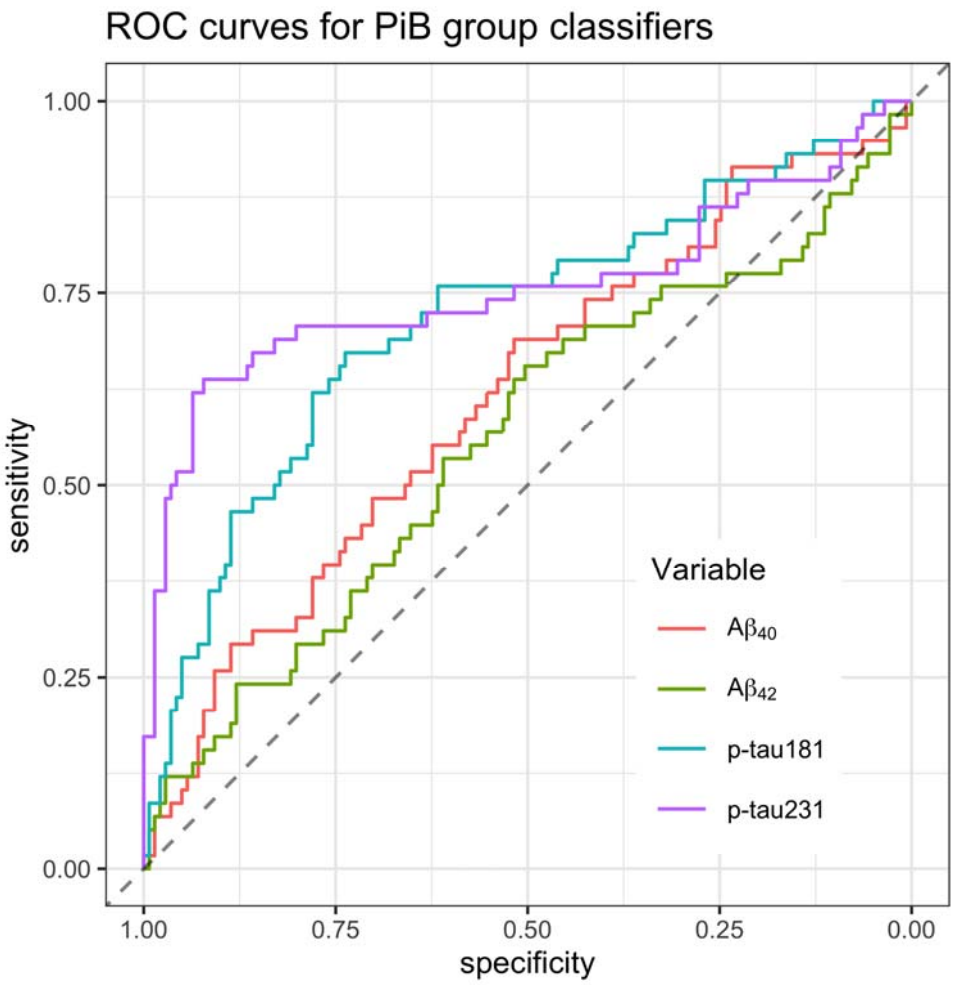

Supplementary Figure 7: Receiver operating characteristic curves for univariate models for predicting PiB group. PiB, Pittsburgh compound B; p-tau, phosphorylated tau; ROC, receiver operating characteristic.

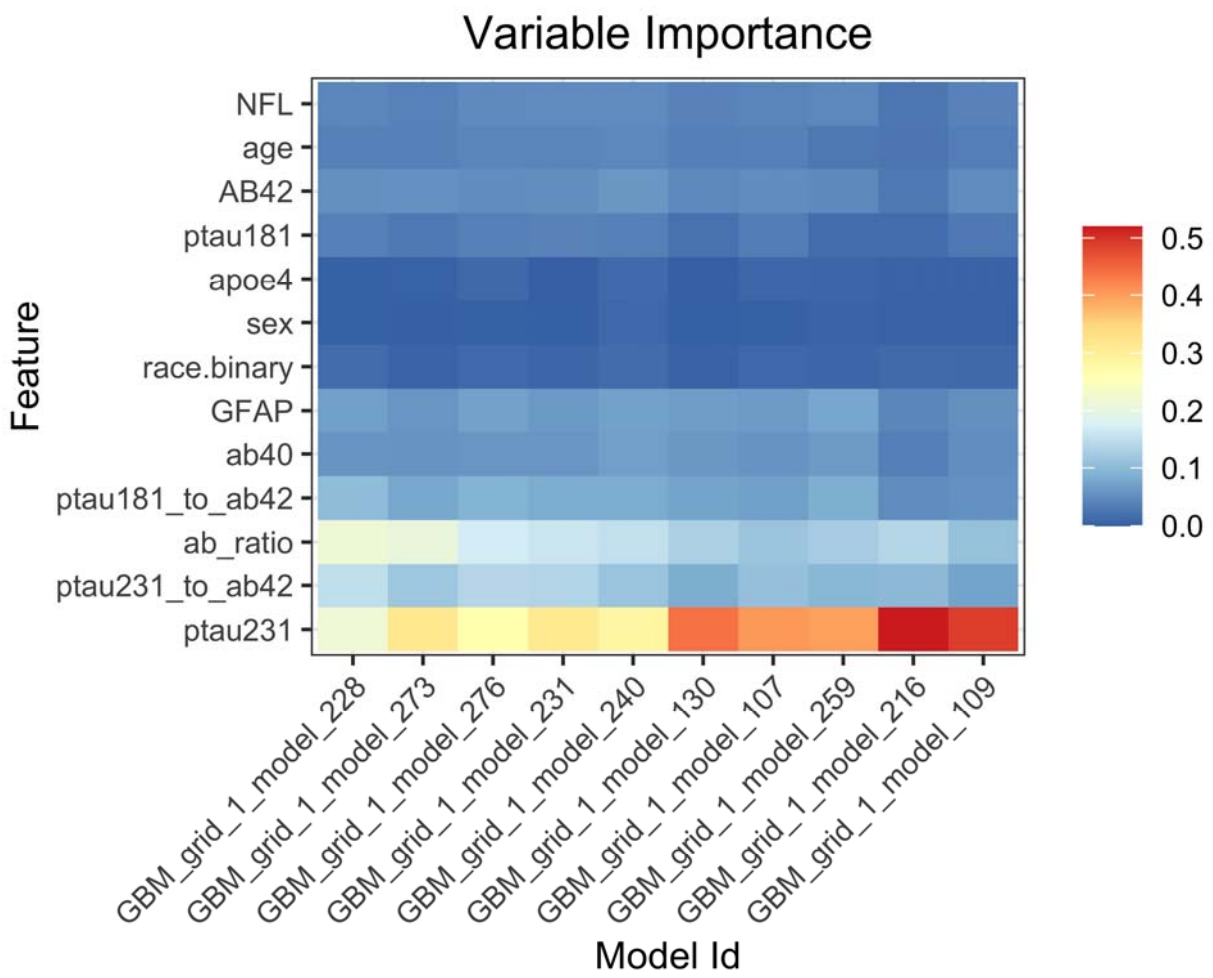

Supplementary Figure 8: Variable importance in the top 10 (based on cross-validation AUC) multivariable models. APOE, apolipoprotein E; GBM, gradient boosting machine; GFAP, glial fibrillary acidic protein; NfL, neurofilament light chain; p-tau, phosphorylated tau.

Longitudinal intraclass correlation coefficients

Supplementary Table 2: *Longitudinal intraclass correlation coefficients.*

Biomarker	Overall		PiB−		PiB+	
	ICC	95% CI	ICC	95% CI	ICC	95% CI
$A\beta_{40}$	0.48	(0.39–0.55)	0.47	(0.35–0.58)	0.64	(0.5–0.75)
$A\beta_{42}$	0.49	(0.41–0.57)	0.59	(0.48–0.68)	0.76	(0.64–0.84)
p-tau181	0.62	(0.55–0.68)	0.61	(0.51–0.7)	0.80	(0.7–0.87)
p-tau231	0.68	(0.61–0.74)	0.61	(0.51–0.7)	0.80	(0.7–0.87)

Abbreviations: Aβ, amyloid-β; cDVR, cortical distribution volume ratio; CI, confidence interval; GFAP, glial fibrillary acidic protein; ICC, intraclass correlation coefficient; NfL, neurofilament light chain; PiB, Pittsburgh compound B; p-tau, phosphorylated tau.

Longitudinal plasma biomarker trajectories by brain amyloid status

Supplementary Table 3: *Linear mixed effects model results for intercept. Standard errors are shown in parentheses. * p < .05, ** p < .01, *** p < .001.*

Biomarker	Model	PiB-	PiB+	Difference
$A\beta_{42}/A\beta_{40}$	Unadjusted	0.0531 (0.000752)***	0.0445 (0.00118)***	-0.0086 (0.0014)***
	Adjusted	0.0527 (0.000741)***	0.0451 (0.00118)***	-0.00758 (0.00141)***
$A\beta_{40}$	Unadjusted	138 (2.81)***	153 (4.46)***	15.5 (5.27)**
	Adjusted	143 (2.31)***	148 (3.71)***	5.29 (4.41)
$A\beta_{42}$	Unadjusted	7.11 (0.125)***	6.63 (0.197)***	-0.485 (0.233)*
	Adjusted	7.27 (0.119)***	6.45 (0.19)***	-0.813 (0.227)***
GFAP	Unadjusted	178 (6.78)***	247 (10.6)***	68.9 (12.6)***
	Adjusted	186 (6.08)***	230 (9.63)***	44.1 (11.6)***
NfL	Unadjusted	23.6 (0.919)***	29.4 (1.44)***	5.87 (1.71)***
	Adjusted	25.1 (0.711)***	26.8 (1.13)***	1.73 (1.35)
p-tau181	Unadjusted	8.21 (0.536)***	12.9 (0.835)***	4.68 (0.992)***
	Adjusted	8.75 (0.472)***	11.9 (0.75)***	3.17 (0.896)***
p-tau181/$A\beta_{42}$	Unadjusted	1.21 (0.074)***	1.99 (0.115)***	0.78 (0.137)***
	Adjusted	1.26 (0.0681)***	1.86 (0.107)***	0.599 (0.129)***
p-tau231	Unadjusted	16.1 (0.705)***	27.1 (1.1)***	11.1 (1.31)***
	Adjusted	16.8 (0.652)***	26.2 (1.04)***	9.41 (1.24)***
p-tau231/$A\beta_{42}$	Unadjusted	2.47 (0.129)***	4.46 (0.2)***	1.99 (0.238)***
	Adjusted	2.51 (0.128)***	4.36 (0.202)***	1.86 (0.243)***

Abbreviations: Aβ, amyloid-β; GFAP, glial fibrillary acidic protein; NfL, neurofilament light chain; PiB, Pittsburgh compound B; p-tau, phosphorylated tau.

Supplementary Table 4: *Linear mixed effects model results for longitudinal rates of change in plasma measures by PiB group. Standard errors are shown in parentheses. * p < .05, ** p < .01, *** p < .001. p-values between .05 and .1 are stated below. p-values greater than .1 are not indicated.*

Biomarker	Model	PiB-	PiB+	Difference
$A\beta_{42}/A\beta_{40}$	Unadjusted	-0.000406 (0.0000946)***	0.000138 (0.000165)	0.000544 (0.00019)**
	Adjusted	-0.000385 (0.0000977)***	0.000156 (0.000167)	0.000541 (0.000195)**
$A\beta_{40}$	Unadjusted	0.362 (0.602)	2.36 (1.03)*	2 (1.2) p = 0.1
	Adjusted	0.656 (0.557)	1.17 (0.966)	0.511 (1.12)
$A\beta_{42}$	Unadjusted	-0.0496 (0.0257) p = 0.06	0.11 (0.0439)*	0.16 (0.0508)**
	Adjusted	-0.0409 (0.0253)	0.0643 (0.0432)	0.105 (0.0504)*
GFAP	Unadjusted	4.92 (1.13)***	9.16 (1.89)***	4.24 (2.21) p = 0.06
	Adjusted	5.51 (1.13)***	7.83 (1.89)***	2.32 (2.23)
NfL	Unadjusted	0.838 (0.173)***	1.54 (0.292)***	0.705 (0.34)*
	Adjusted	0.917 (0.165)***	1.14 (0.279)***	0.22 (0.327)
p-tau181	Unadjusted	0.0433 (0.0949)	0.502 (0.152)**	0.458 (0.18)*
	Adjusted	0.0791 (0.0943)	0.426 (0.157)**	0.347 (0.183) p = 0.06
p-tau181/$A\beta_{42}$	Unadjusted	0.00397 (0.017)	0.0602 (0.0273)*	0.0562 (0.0321) p = 0.08
	Adjusted	-0.000981 (0.0174)	0.0653 (0.028)*	0.0663 (0.0336) p = 0.05
p-tau231	Unadjusted	0.339 (0.146)*	0.957 (0.236)***	0.618 (0.277)*
	Adjusted	0.382 (0.143)**	0.756 (0.24)**	0.373 (0.278)
p-tau231/$A\beta_{42}$	Unadjusted	0.0251 (0.0261)	0.112 (0.0425)**	0.0871 (0.0499) p = 0.08
	Adjusted	0.0229 (0.0268)	0.11 (0.0439)*	0.0874 (0.0525) p = 0.1

Abbreviations: Aβ, amyloid-β; GFAP, glial fibrillary acidic protein; NfL, neurofilament light chain; PiB, Pittsburgh compound B; p-tau, phosphorylated tau.

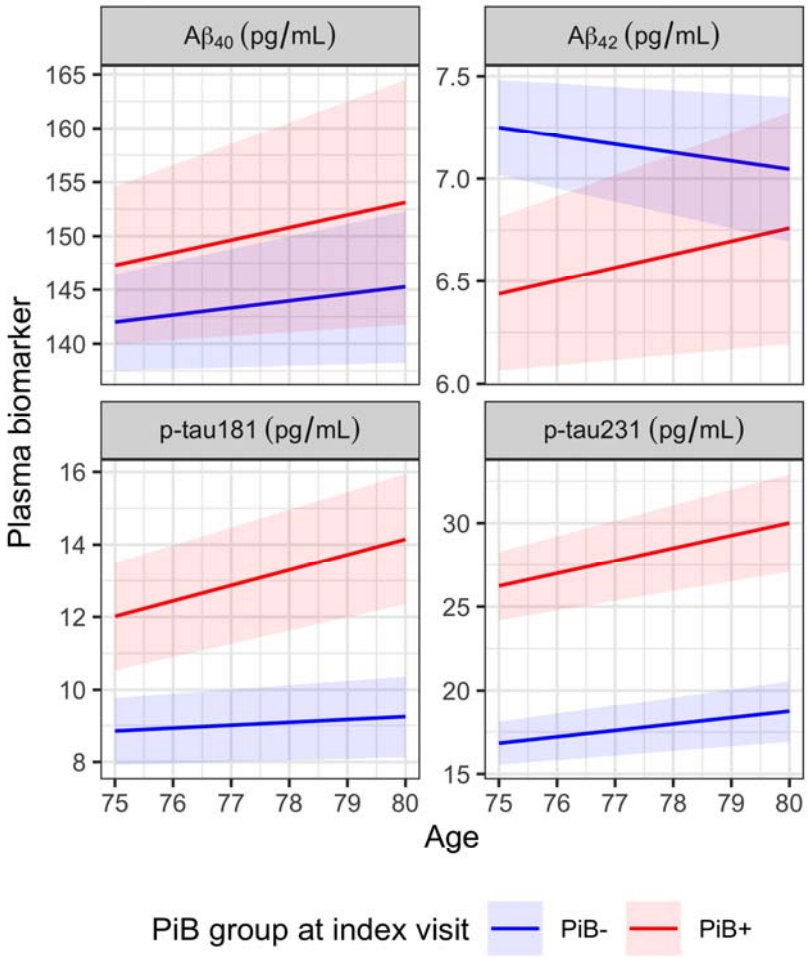

Supplementary Figure 9: Predicted plasma biomarker trajectories for A , A , p-tau181, and p-tau231. PiB, Pittsburgh compound B; p-tau, phosphorylated tau.

Associations among longitudinal rates of change in plasma biomarkers and brain amyloid

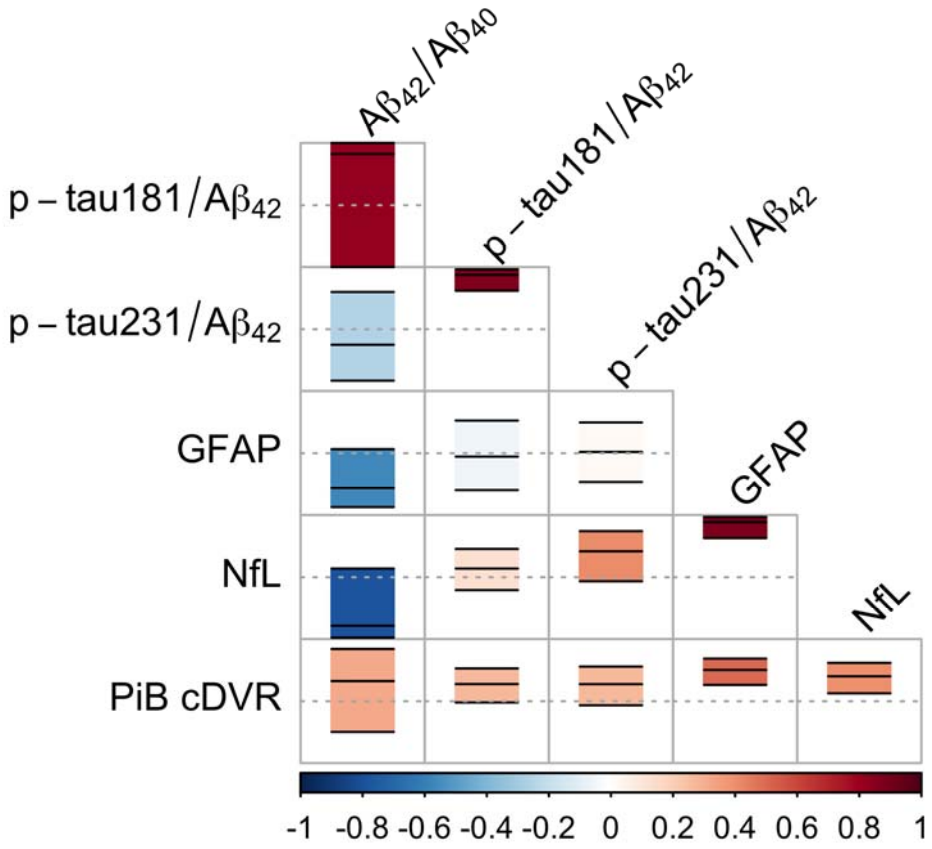

Supplementary Figure 10: Pairwise correlations among rates of change of plasma and PiB PET measures, as assessed using the random effect correlation matrix estimated in the bivariate linear mixed effects models. The rectangle in each cell indicates the 95% confidence interval of the correlation estimate, which is shown with a black solid line inside the rectangle. Dashed horizontal lines correspond to a correlation of 0. Color indicates the correlation estimate. cDVR, cortical distribution volume ratio; GFAP, glial fibrillary acidic protein; NfL, neurofilament light chain; PiB, Pittsburgh compound B; p-tau, phosphorylated tau.

Temporal order of changes in plasma biomarkers and brain amyloid

Progression score model

The progression score (PS) model used in our analysis is given by

$$
\begin{aligned}
s_{ij} &= t_{ij} + \tau_i \\
y_{ijk} &= a_k \operatorname{logit}^{-1}\big(b_k(s_{ij} - c_k)\big) + d_k + \epsilon_{ijk} \\
\tau_i &\sim \mathcal{N}(0, \sigma_\tau^2) \\
\boldsymbol{\epsilon}_{ij} &\sim \mathcal{N}(0, \boldsymbol{\Sigma}),
\end{aligned}
$$

where t_{ij} is age (or time) of subject i at visit j, τ_i is the time-shift for this subject, s_{ij} is the PS at this visit, y_{ijk} is the measurement for k^{th} biomarker at this visit, $\{a_k, b_k, c_k, d_k\}$ are sigmoid trajectory parameters for this biomarker, and ϵ_{ijk} is random noise. The modeling of correlations among biomarkers through the covariance matrix $\boldsymbol{\Sigma}$ ensures that PS will not be unduly influenced by overlapping information conveyed by the biomarkers.

For simplicity in model fitting, we assumed that all biomarker trajectories were increasing, which allowed us to use more specific hyperpriors for the sigmoid to guide parameter estimation. (Given this assumption, $\text{A}\beta_{42}/\text{A}\beta_{40}$ values were negated prior to model fitting, and results were transformed back to the original scale of the biomarker.)

Selection of hyperpriors were guided in part by [32] and the Bayesian linear regression implementation in rstanarm. Hyperpriors for the sigmoid parameters were

$$
\begin{aligned}
a_k &\sim \text{Half-}\mathcal{N}(3.92\,\sigma_{y_k}, \sigma_{a_k}^2) \\
b_k &\sim \text{Half-}\mathcal{N}(0, \sigma_{b_k}^2) \\
c_k &\sim \mathcal{N}(0, (3\sigma_t)^2) \\
d_k &\sim \mathcal{N}(\mu_{y_k} - 1.96\,\sigma_{y_k}, \sigma_{a_k}^2),
\end{aligned}
$$

where μ_{y_k} and σ_{y_k} are the mean and standard deviation of the kth biomarker, respectively, σ_t is the standard deviation of the time variable t (across all subjects and visits), $\sigma_{a_k} = 1.5\,\sigma_{y_k}$, and $\sigma_{b_k} = 1/\sigma_t$.

The biomarker residual covariance matrix was parameterized using $\Sigma = \Lambda C \Lambda$, where Λ is a diagonal matrix with positive diagonal entries and C is a positive-definite correlation matrix with the following priors:

$$\begin{aligned} [\Lambda]_{kk} &\sim \text{Exp}(\sigma_{y_k}^{-1}) \\ C &\sim \text{LKJ}(1). \end{aligned}$$

For the standard deviation of the subject-specific time-shift, we used the hyperprior $\sigma_\tau \sim \text{Half-Cauchy}(0,5)$.

We estimated model parameters using Hamiltonian Monte Carlo Markov chain with 4 chains and 10,000 warm-up samples followed by 5000 posterior draws per chain using RStan [40]. There were no divergent transitions after warm-up. Maximum $\hat{R}$ was 1.02, indicating model convergence.

Time interval between peak relative change in plasma biomarkers and amyloid positivity onset

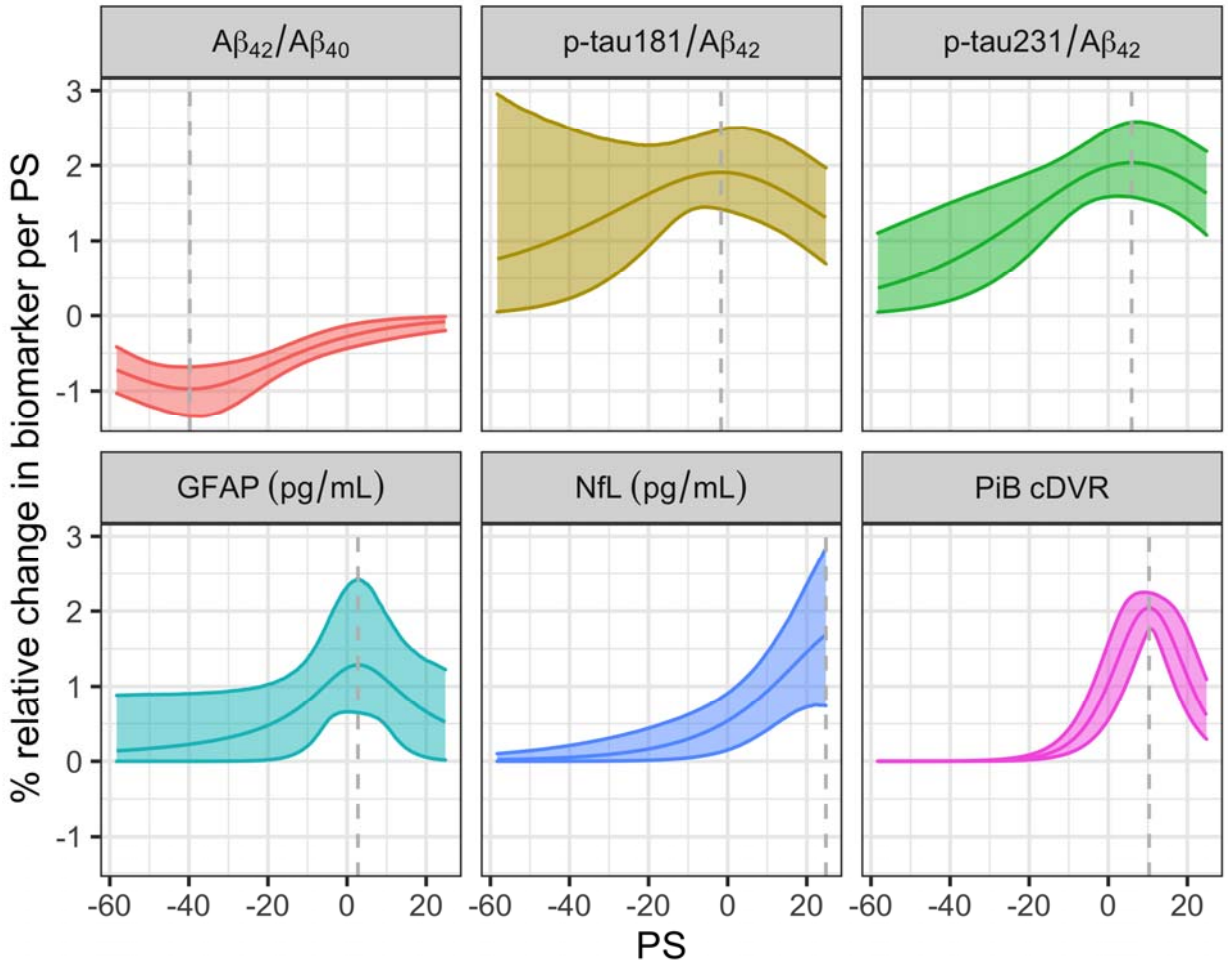

Supplementary Figure 11: Percent relative change in biomarkers per PS as a function of PS. Bands indicate 95% confidence intervals. Vertical dashed lines indicate the PS at which absolute percent relative change is maximal.

Supplementary Table 5: *Peak percent relative biomarker change (per year) and time interval (in years) between peak relative change and the PS value that corresponds to PiB positivity threshold.*

Biomarker	Peak % relative change	Interval between peak and amyloid onset
$A\beta_{42}/A\beta_{40}$	-0.99 (-1.37, -0.69)	-41.3 (-53, -31.7)
p-tau181/$A\beta_{42}$	1.96 (1.56, 3.45)	-5.1 (-37.6, 12.1)
p-tau231/$A\beta_{42}$	2.08 (1.63, 2.64)	4.7 (-10.9, 15.5)
GFAP	1.42 (0.74, 2.68)	1.5 (-26, 18)
NfL	1.98 (0.88, 3.46)	17.9 (-11.8, 27.1)
PiB cDVR	2.11 (1.95, 2.28)	10.1 (9.1, 11.2)

Abbreviations: Aβ, amyloid-β; cDVR, cortical distribution volume ratio; GFAP, glial fibrillary acidic protein; NfL, neurofilament light chain; PiB, Pittsburgh compound B; p-tau, phosphorylated tau.